

UNIVERSITÀ DEGLI STUDI DI NAPOLI FEDERICO II

DIPARTIMENTO DI STRUTTURE PER L'INGEGNERIA E
L'ARCHITETTURA

TESI DI LAUREA SPECIALISTICA IN
INGEGNERIA STRUTTURALE E GEOTECNICA



**VISK: A GIS-COMPATIBLE PLATFORM FOR
MICRO-SCALE ASSESSMENT OF FLOODING RISK
IN URBAN AREAS**

Relatore:

Ch.mo Prof. Ing. Gaetano Manfredi

Correlatori:

Ing. Fatemeh Jalayer
Ing. Raffaele De Risi

Candidato:
Stefano Carozza
Matr. 344/196

Anno Accademico 2012/2013

*In Memoria di
Nello e Daniel*

Acknowledgements

Mi accingo a scrivere queste righe a pochi giorni dalla tanto ambita laurea e questo è sicuramente uno dei periodi più intensi della mia carriera universitaria: pieno di impegni, scadenze, emozioni, in cui la gioia per il traguardo che sto per raggiungere si alterna a momenti di malinconia nei quali ricordo e ripenso, con rammarico, a tutte le meravigliose esperienze che mi lascio alle spalle.

Il mio primo pensiero non può che essere rivolto al neo phD Raffaele De Risi che da qualche anno mi onora della sua amicizia, fondamentale per me in tantissimi momenti. Il suo sapere, le sue indiscutibili capacità e la sua umiltà nel porsi di fronte alle problematiche sono state per me un modello ed un incoraggiamento a migliorarmi sempre di più. Lo ringrazio per la fiducia che ha riposto in me e per tutto ciò che mi ha dato dal punto di vista intellettuale ed umano. Spero con tutto il cuore di continuare a collaborare con lui e, che la nostra amicizia accresca sempre di più negli anni a venire.

Un altro ringraziamento speciale voglio esprimere nei confronti di Fatemeh Jalayer, una ricercatrice esemplare e degna di ammirazione. La ringrazio per la possibilità e la fiducia che mi ha dato, per avermi fatto conoscere ed approfondire alcune tematiche così affascinanti e, per aver contribuito profondamente ad accrescere la mia modesta preparazione.

Ringrazio il prof. Gaetano Manfredi che, dai tempi del corso di Tecnica delle Costruzioni ad oggi, mi ha trasmesso innumerevoli conoscenze, lasciando impresse nella mia memoria le qualità che maggiormente lo distinguono: la conoscenza, l'intuito e la lungimiranza, che fanno di lui uno dei personaggi più illustri della comunità scientifica.

Voglio ricordare e nel contempo ringraziare i professori G.M. Verderame, N. Augenti, E. Cosenza, R. Ramasco, G. Della Corte, E. Nigro, A. Prota, G. Magliulo e G. Serino per tutto ciò che mi hanno insegnato con le loro affascinanti ed indimenticabili lezioni. Con loro ringrazio anche i tantissimi ricercatori, phD e dottorandi che negli

Acknowledgements

anni hanno tenuto esaustive esercitazioni, tra i quali ricordo: C. Galasso, F. De Luca, G. Lignola, M. Polese, D. Cancellara, F. Parisi e M. Di Ludovico.

L'università mi ha dato l'opportunità di conoscere tantissime persone straordinarie che hanno allietato i momenti difficili e reso più piacevoli questi anni trascorsi insieme. Ringrazio tutti i miei compagni di corsi, e le persone con le quali ho condiviso le gioie e i dolori delle attività di gruppo. Tra i tanti voglio ricordare, con particolare affetto, Marco G., Michele R., Gaetano A., Crescenzo P., Marianna E., Maddalena C., Simona L., Francesco I., Fabio G., Ciro P., Giuseppe I., Giuseppe M., Nicola S., Pietro L.

Un pensiero doveroso va ai fraterni amici, che per anni mi hanno supportato emotivamente e fatto da "sfogo" per lo stress accumulato in facoltà. Abbraccio calorosamente Fiorentino, Francesco, Amedeo e Alfredo, futuro validissimo ingegnere.

Fondamentale per me in questo lungo e tortuoso percorso è stata la mia famiglia. Il mio papà Vincenzo, mio mentore da sempre che, nonostante i suoi lunghi (e talvolta estenuanti!) discorsi, sarà sempre per me un modello di vita e di rettitudine; la mia mamma Emilia, donna di dolcezza, devozione e pazienza infinita, che ancora oggi con i suoi sguardi alimenta la mia linfa vitale; la mia sorellina Angela, che ormai vedo così grande e matura, è stata spesso per me una sorella maggiore più di quanto lo sia stato io per lei, la amo e rappresenta per me un modello da seguire per la sua grandissima forza di volontà e la tenacia che esterna in tutto ciò che fa. Ringrazio i miei nonni: Stefano per gli insegnamenti di vita, Vincenza per i sostanziosi pranzi (fonte di energia per lo studio), Michele per gli esilaranti racconti e Angelina per aver educato la mamma migliore che potessi avere. Un grazie ai miei numerosi zii e cugini tra i quali, con particolare gioia, voglio ricordare zia Angelina e zio Angelo, i miei secondi genitori e Maria e Francesco che, non ho mai considerato cugini, ma sempre fratelli.

Voglio ringraziare anche tutte le persone che mi hanno demotivato, deluso e che mi hanno fatto soffrire soprattutto in quest'ultimo periodo. Le ringrazio perché attraverso la loro presenza ho potuto dimostrare la mia forza, le mie capacità ed ho potuto accrescere la convinzione in ciò che faccio ed in cui credo.

Il ringraziamento più grande però voglio esternarlo a Dio. Lo ringrazio con tutto me stesso per avermi fatto così come sono, per avermi dato ciò che ho, per avermi dato la

Acknowledgements

fede, la mia famiglia, i miei amici, per avermi fatto amare l'ingegneria e per le passioni che ho coltivato. Lo ringrazio per le difficoltà e le prove alle quali mi ha sottoposto e che mi ha aiutato sempre a superare, per le gioie, i dolori e per l'amore che ha verso noi tutti ma, soprattutto, Lo ringrazio perché ha sempre esaudito i miei bisogni e non ha mai vanificato le mie preghiere.

03/07/2013

Stefano

Abstract

The evaluation of flooding risk in urban areas is an useful research argument with the purposes both of the mitigation of the problem related to the flooding damages and the improvement of the urban planning that take into account the climate changes.

Risk assessment may be executed in two temporal scale (short- and long-term) and in two spatial scale (meso- and micro-scale). This thesis is focused on the risk assessment evaluated in micro-scale and in long-term for the urban contests of a group of buildings with an uncorrelated structural response (portfolio of buildings) members of the same class (i.e., buildings with homogeneous characteristics).

The flood risk assessment problem is composed of three sub-classes of problems that are: hazard, vulnerability and exposure.

The micro-scale hazard assessment provides to evaluate the maximum values of flooding height and velocity for a series of given return periods spatially related to a lattice of points above the interest zone. To arrive at this result the methodology starts to the definition of historical rainfall data and their projections in future climate change. Through the knowing of the rainfall curves (IDF - Intensity Duration Frequency), the topography, the geology and the land use of the area of interest it is possible to obtain the hydrograph curves that represents the discharge water volume for the given return periods. With the hydrograph and a topographical digital elevation model (DEM) it is possible, through the software FLOW-2D®, to diffuse spatially the entire flow rate in the area of interest in order to evaluate the hazard profile in terms of water height and velocity. To reduce the number of variable that regard the problem, water velocity is approximate as a power law of the height profile, so that only water height is used as interactive variable during the calculations.

Flooding vulnerability assessment occur through a Bayesian and simulated-based algorithm that due to evaluate the capacity of the class of building respect to flooding problem. The methodology have the purpose to characterize the structural fragility function through the assigning of uni- and

Abstract

bi-modal probability distributions regards the uncertain parameters that define the structures. The calculation of the fragility function is achieved with a small numbers (about 50) of Monte Carlo simulations to define the structural models to submit to analysis procedure. This last is performed on bi-dimensional models evaluated with the finite-elements method through the open source software named OpenSees. The structural models include the presence of the openings (doors and windows) and their waterproof capacity. The analysis procedure take in to account the various sources of uncertainty produced by the different details and geometry observable building-to-building, the not-complete knowledge of the mechanical property of the materials and the characteristics of the flooding load. The uncertain parameters may be divided in discrete binary variables (logic statement) or continuous uncertain variables. The extraction on the probability that the first category of uncertain parameters have to realize, due to establish in a logic tree approach the kind of model on which apply the analysis procedure. Instead, the extraction on the value that continuous parameters have (given a probability distribution) confers the dimensions and the mechanical property of the selected model. The vulnerability of the class of buildings, in end, is represented as the *robust fragility curves* calculated as statistics (16th, 50th and 84th percentile) of a set of plausible curves calculated considering the mentioned uncertainty.

Flooding micro-scale risk assessment of a portfolio of building is performed through the building-to-building integration of the flooding hazard curves and the robust fragility curves. Flooding risk is expressed in different modes: the mean annual frequency of exceeding a given limit state, the probability of exceeding a limit state in a given number of years, the expected number of casualties and the expected replacement/reconstruction costs.

The entire methodology of micro-scale vulnerability and risk assessment is implemented in a Matlab®-based graphic user interface that composes the GIS-based software platform developed during this thesis work named VISK (acronym of Visual Vulnerability and flooding rISK). This software allows to execute a vulnerability and risk assessment as above explained with the automatic management of the uncertain parameters and structural models. The vulnerability assessment, in the specific of the structural analysis is performed with the open source code OpenSees. VISK also allows the input of different types of customs fragility curve as expression of user-defined flooding

Abstract

vulnerability of the buildings. The GIS compatibility produces a series of advantages, for example, allows the graphical input and output and providing an efficient visualization of the flooding risk. VISK gives the possibility to view the results both in a detailed scale (building-to-building) and as overall estimates of the entire area.

An application of the flooding vulnerability and risk assessment methodology is applied on the case study of Suna (Dar Es Salaam in Tanzania) through the VISK platform in consideration of the European FP7 project CLUVA (Climate Change and Urban Vulnerability in Africa). In this contest the portfolio of buildings is composed by a class of informal settlements (i.e. not engineered constructions). This last are particularly sensible to flooding problem because one of their peculiarity is that they are a direct product of the rapid and un-programmed urbanization that often occur in flood-prone areas and are constructed without formal engineering criteria.

Keywords: VISK, flood, hazard, fragility, vulnerability, exposure, risk assessment, bayesian framework, flood prone, gis.

Table of contents

CHAPTER 1

INTRODUCTION	15
1.1 OBJECTIVES.....	16
1.2 BACKGROUNDS AND PRELIMINARY KNOWLEDGE.....	16
1.3 OUTLINES	17
1.4 CASE STUDY	18

CHAPTER 2

METHODOLOGY.....	21
2.1 INPUT DATA	22
2.1.1 Orthophotos and footprint of the buildings.....	22
2.1.2 Hydraulic results and flooding hazard curves	24
2.1.3 Characterization of uncertainties and logic-trees approach.....	28
2.2 VULNERABILITY AND RISK ASSESSMENT	32
2.2.1 Limit states definition	32
2.2.2 Flood action	33
2.2.3 The structural modelling	36
2.2.4 The structural analysis	38
2.2.5 The analytical fragility curves	40
2.2.6 The robust fragility estimation.....	43
2.2.7 Risk assessment	44

CHAPTER 3

INTRODUCTION TO VISK	47
3.1 INTERFACE DESCRIPTION	48
3.2 VIISK MANUAL.....	55
3.2.1 Workspace initialization.....	56
3.2.2 Buildings vulnerability assessment	57
3.2.3 Risk assessment	58
3.3 VIISK STRUCTURAL ANALYSIS PROCEDURE	58
3.4 VIISK VULNERABILITY AND RISK ASSESSMENT	60
3.4.1 Robust fragility curve	60
3.4.2 Others fragility curve	62
3.4.3 Risk integration	63

Table of contents

CHAPTER 4

CASE STUDY: SUNA.....	65
4.1 HAZARD FLOODING DEFINITION.....	66
4.1.1 <i>The IDF curve: historical and climate projections data</i>	66
4.1.2 <i>Catchment area and hydrographs definition</i>	67
4.1.3 <i>Micro-scale flood hazard</i>	68
4.2 CHARACTERIZATION OF UNCERTAINTIES	71
4.3 VULNERABILITY ASSESSMENT: ANALYSIS AND FRAGILITY CURVES.....	75
4.3.1 <i>Effect of analysis number in vulnerability assessment</i>	76
4.3.2 <i>Effect of extraction criteria in vulnerability assessment</i>	78
4.3.3 <i>Effect of distributions probability in vulnerability assessment</i>	80
4.3.4 <i>Effect of water load in vulnerability assessment</i>	82
4.4 RISK ASSESSMENT	89

CHAPTER 5

FINAL REMARKS	93
REFERENCES	99
LIST OF FIGURES	101
LIST OF TABLES	103

Chapter 1

INTRODUCTION

In the last years about the 70-90 percent of natural disasters such as storms, droughts, floods and landslides are related to climate change. In particular, only in the first semester of the 2012, about 35% of natural disaster were related to flood. This phenomenon in added to the rapid rate of urbanization leads to increase the exposure to risk in urban areas.

Flooding disaster in the first semester of 2012 represent the 62% of total people affected and the 10% of total economic losses due to natural disaster.

To programming a flooding risk mitigation, through an optimal urban planning targeted to reducing the victims of flooding disaster and the structural problem at affected buildings, we need of an instrument that allow to calculate the flooding risk in urban areas related to climate change.

1.1 Objectives

The general objective of this thesis is the study and the development of a GIS-compatible platform for flood risk assessment for individual buildings located in homogenous urban areas with a micro-scale valuation. This platform is named VISK and its main prerogatives are follows explained.

Interactively and user friendly interface. The platform may be used also from not-expert people in risk assessment.

Visual input/output interaction. To confers at the users a good capacity of control of the entire procedure and the results, and an easily implementation of all the data necessary to the various evaluations.

Exportability of results. The results must be able to be reused in other software platform GIS-compatibles. This aspect confers to VISK a large elasticity because its results may be interfaced with other software.

Customizability. Users must be able to choice the options related to various aspect of the methodology (e.g., kind of probability distribution, water load, fragility type, etc.).

All these purposes are been at the centre of all the programming phases and interface design to ensure a good user experience of the software.

1.2 Backgrounds and preliminary knowledge

To realize the platform to risk assessment are been necessary a series of preliminary studies. At first it was necessary to elaborate a methodology and a mathematical model of the entire procedure that starting from the definition of the problem may lead to the resolution of the same.

The work is started with a data recognition and a depth study of the flooding problem from the hydraulic point of view, the preliminary definition of the *rainfall curves* and how it is possible to realize a *hydrograph curve* through the geology and land use maps and the topography of the area of interest. This phase is been very important because it is been necessary to characterize the *flooding hazard assessment*.

Simultaneously also the geo-referred photo, and their matrix computerized treatment, are studied. This to have a good knowing about the potentiality of GIS information in the resolution of engineering problems. In fact, using a geo-

referred photo and GIS procedures, it is possible to confer a visual aspect to a mathematical problem that include a geographic map. Through this study is been realized a *stratified information system* that allows the graphical representation of hazards maps, buildings and more other information in an overlapping view on the geographic map.

The approach of the methodology used to risk assessment is semi-probabilistic-based so that an exhaustive study of the probability and statistic it was necessary.

From the structural point of view the preliminary knowledge necessary to resolve the risk assessment problem regards the evaluation of the capacity of the building respect at the flooding load path. The result of this evaluation is the *fragility curve*.

The study of the *risk calculation* and its expressions and means is been fundamental for the realization of the platform.

All the topics listed above regard only the methodological aspect of the risk assessment problem. To realize the software platform is been necessary to deepen the knowing about the *Intelligence Development Environment (IDE)* of Matlab® programming language to manage the GIS-platform and OpenSees code to execute the structural analysis. Regarding Matlab®, a study of the Graphic User Interface implementation is leaded in add to the knowing of all the GIS functions and programming procedures necessary to obtain an efficacy assessment platform. In end, OpenSees code, is been studied to realize efficacy structural models and to execute the analysis that allow the realization of the fragility curves.

1.3 Outlines

This thesis starting with this *introductive chapter* (**Chapter 1**) in which the scopes, the objectives and the preliminary knowledge are explained.

In **Chapter 2** the *methodology* used to execute the risk assessment is presented; all the phases of the methodology are reported with a focalization on the various aspect that regards input data, orthophoto, hazard definition starting from the definition of flooding load, limit states, structural models, characterization of the uncertain parameters, structural analysis, vulnerability evaluation, robust fragility and risk integration.

After the methodology VISK platform are introduced (**Chapter 3**). In this chapter are presented the interface of the software, a little guide to use VISK (in which is explained how to initialize the workspace, how to execute vulnerability and risk assessment), the procedure with which VISK elaborate the structural analysis (using OpenSees code), the fragility curves and the risk maps.

In **Chapter 4** an example of the entire procedure is reported on a case study (Suna in Dar Es Salaam). A numerical example of all the phases are described, from the data acquiring to the risk evaluation.

A conclusive chapter (**Chapter 5**) concludes this thesis. In this chapter a summary of the entire thesis is reported with a synthesis of the main results presented and the possible future developments of VISK platform.

1.4 Case study

The application of the methodology through the software developed in this thesis is demonstrated for the urban context of Dar Es Salaam (Tanzania) where a complete risk assessment procedure is carried out for the informal settlements in the neighbourhood of Suna.

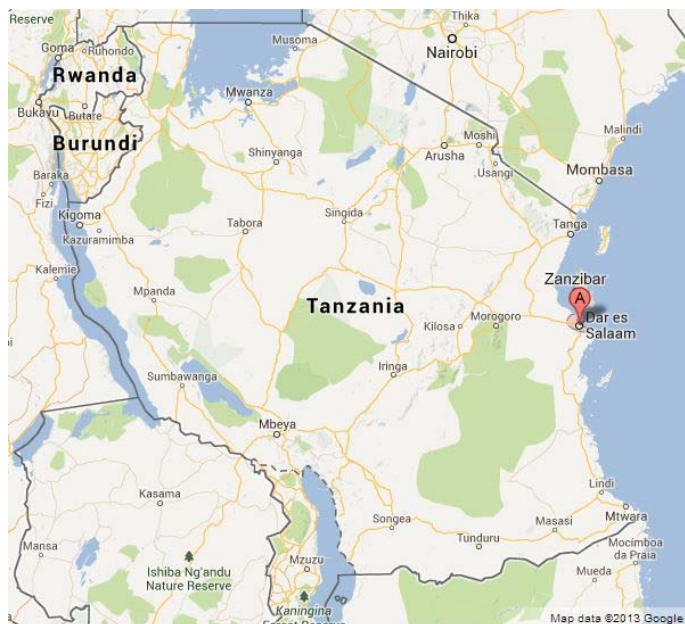


Figure 1. 1- Dar Es Salaam in Tanzania

Introduction

The city of Dar Es Salaam (DSM) in Tanzania is located between latitudes 6.36° and 7.0° to the South of Equator and longitudes 39.0° and 33.33° to the East of Greenwich. It borders Indian Ocean on the east and its coastline stretches about 100km between the Mpiji River to the north and the Mzinga River in the south.

The total surface area of Dar Es Salaam city is about 1800 km^2 , comprising of 1393 km^2 of land mass with eight offshore islands, which is about 0.19% of the entire Tanzania Mainland's area. Administratively, Dar es Salaam City is divided into three municipalities and Districts of Kinondoni, Ilala and Temeke, with a total population of 2698651 according to the 2005 population census.

Chapter 2

METHODOLOGY

In this Chapter is explained the new probabilistic based methodology for flooding vulnerability assessment for a portfolio of buildings. This last is a group of building with an uncorrelated structural response and they also may be divided in classes of buildings with homogeneous characteristics.

The flood vulnerability for a class of structures is evaluated analytically by means of an efficient Bayesian simulated-based methodology. This methodology is based on a thorough characterization of the various sources of uncertainty such as build-to-building variability within a given class, uncertainty in loading parameters, and uncertainty in material mechanical properties.

The flood vulnerability for a class of structures is represented by the “fragility curves” (and its plus/minus one standard deviation confidence interval) for a given limit state. The “fragility curves” are defined as the probability distributions (CDF, Cumulative Distribution Function) for the critical water-height marking the threshold of the limit state under consideration. As a results, the critical water height values corresponding to prescribed limit states, may be obtained based on, structural analysis, geometrical characteristics and nominal values.

2.1 Input data

For the application of the proposed methodology are necessary many information and data sets to have a good characterization of the problem. The input data required are: the geo-referred orthophoto of the case study area, the layer of the footprints of the buildings, the flooding height/velocity profiles for prescribed return periods and the uncertainties in structural modelling parameters related to both material mechanical properties and construction details and geometry.

2.1.1 ORTHOPHOTOS AND FOOTPRINT OF THE BUILDINGS

Orthophotos are particular kind of photos that represents a geographic area. They are obtained by assembling areal photos strips together and removing the topographic and geometric distortion by means of an orthorectification instruments. The areal photos are taken in a sequential manner with a constant time interval through a special camera locate on an airplane.

An orthophoto may returns a lot of information if it have a good resolution and if it is geo-referred in one of the many possible geographical reference systems.

The resolution (at least 300 – 600 dpi) confers the possibility of identify with major precision the geometrical details of the buildings represented. If the resolution of orthophoto is very low, the sizes of buildings taken from the photo are affected by an important error because the pixel that represent the vertexes of buildings are not well defined.

Geo-referred orthophotos may be opened with a GIS-compatible program to have the geographical coordinates of all points of the photos in one of the many possible geographical coordinate systems. The information that confers at orthophoto the geo-referred property are content in a *World File* associated ad the image file (the extension is *.tfw* if the orthophoto is in *TIFF* format). This file contains a 3×2 matrix so composed:

$$R = \begin{vmatrix} B & E \\ A & D \\ C & F \end{vmatrix} \quad (2.1)$$

- A: horizontal resolution of the individual pixels (in meters);
- B, D: factors of rotation;

- C, F: translation factors or cartographic coordinates of the pixels in the upper left corner of the raster image (in meters);
- E: vertical resolution of the individual pixels (negative, in meters).

The equations that govern the transformation of image coordinates in geographic coordinates are the sequent:

$$\begin{aligned} X &= A \cdot x + B \cdot y + C \\ Y &= D \cdot x + E \cdot y + F \end{aligned} \quad (2.2)$$

Where (X, Y) are the geographic coordinates in meters and (x, y) are the image coordinates in pixel.

In the practical cases we have two possibility:

- the map image and the World File are available;
- only the map image is available.

In the second case is necessary to georeferencing the map image through the calculation of the elements in the matrix. To calculate these elements, it is necessary to know the image coordinates and the geographic coordinates of three different points of the map and through the application of the equations (2.2) we can determine the elements of the matrix R.

Starting from the geo-referred orthophoto, the user, with a GIS-compatible program as ArcMAP® or VISK, may extracts all buildings footprints with the related geometrical and geographical information and stores these dataset of information in a GIS shape file format. This file can be improved with other information related the buildings, for example it may contains information about the flooding hazard values (in terms of maximum water height and velocity for a set of given return periods) in proximity of buildings.

Figure 2. 1 represents in a schematic mode the sequence of operations that allow the extraction of the buildings footprints from the orthophoto.

For each building identified through the boundary recognition on a geo-referred orthophoto are saved, into the shape file associated, the coordinates of the vertices and the centroid point, the sizes of the sides and the footprint area value. All these data are necessary in the later phases of calculation to the vulnerability and risk assessment.

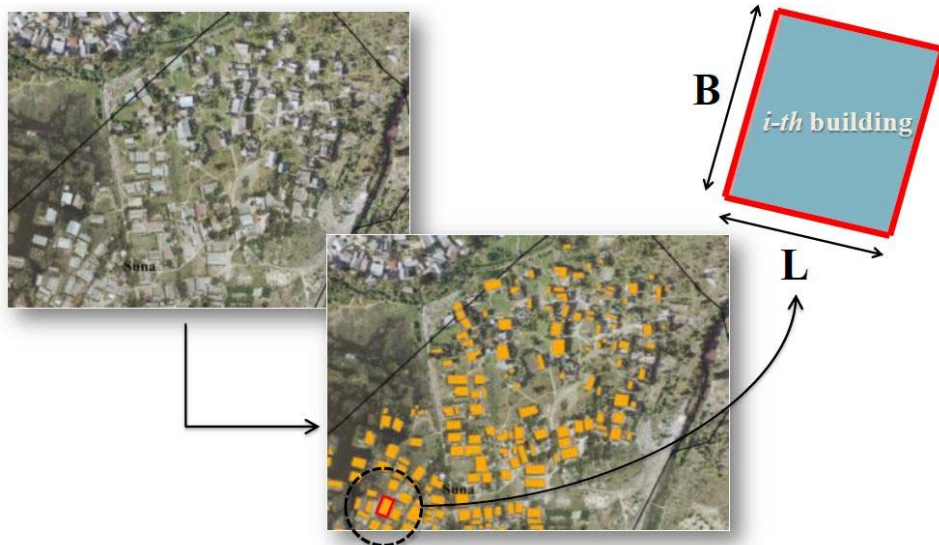


Figure 2.1: Acquisition of data regarding buildings footprint.

2.1.2 HYDRAULIC RESULTS AND FLOODING HAZARD CURVES

Inundation profiles, calculated for various return periods, are one of the main input data for the risk assessment methodology. The inundation profiles are generally expressed in terms of flood depth and velocity, for different return periods of the extreme precipitation event, for each node within a lattice that cover the entire case study area. This information is usually obtained through a general hydrologic/hydraulic routine.

Hydraulic data recognition starts by the definition of a rainfall curves called also IDF curves (Intensity Duration Frequency). These curves present, in particular, the probability of a given rainfall intensity and duration expected to occur in a particular location. Rainfall curve, corresponding to a specific return period, is calculated by fitting a suitable probability model to the extreme rainfall data. An example of the characterization of IDF curve is presented in the expression (2.3):

$$h_r(d, T_R) = a(T_R) \cdot d^n \quad (2.3)$$

in which T_R is the return period, d is the duration, $a(T_R)$ and n are the parameters that have to be estimated through the probabilistic approach.

When IDF curves are estimated the hydrograph curve may be calculated through the procedure illustrated in the schematic diagram of Figure 2.2.

Methodology

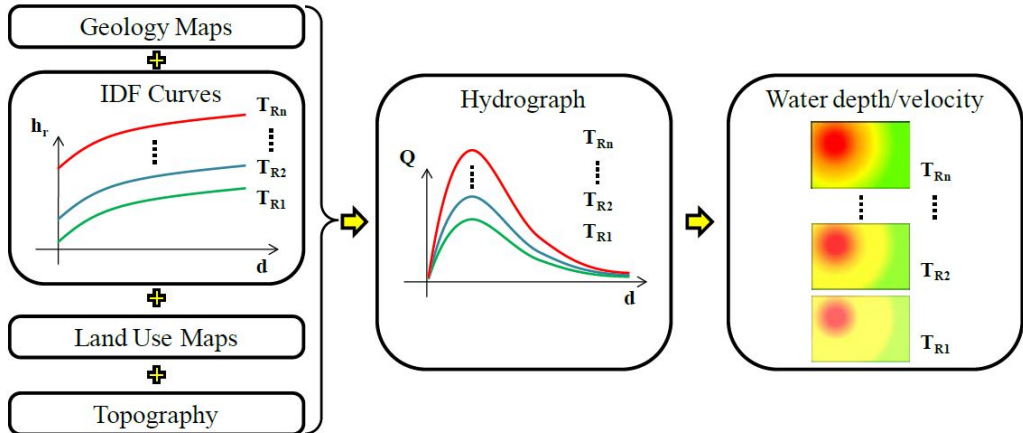


Figure 2.2: Hydrographic basin modelling procedure.

The hydrograph curve is the discharge (volume/time) plotted versus time. As it can be observed in the Figure 2.2, IDF curves, geologic, topography and land-use information are used to characterize the hydrograph leading to the calculation of the total water volume discharged (denoted by Q) for different return periods. This information, together with the topographic map of the zone of interest are used in a two-dimensional diffusion model in order to generate the maps of maximum water height and velocity for each node of a lattice covering the zone of interest for a given return period (the flood hazard map).

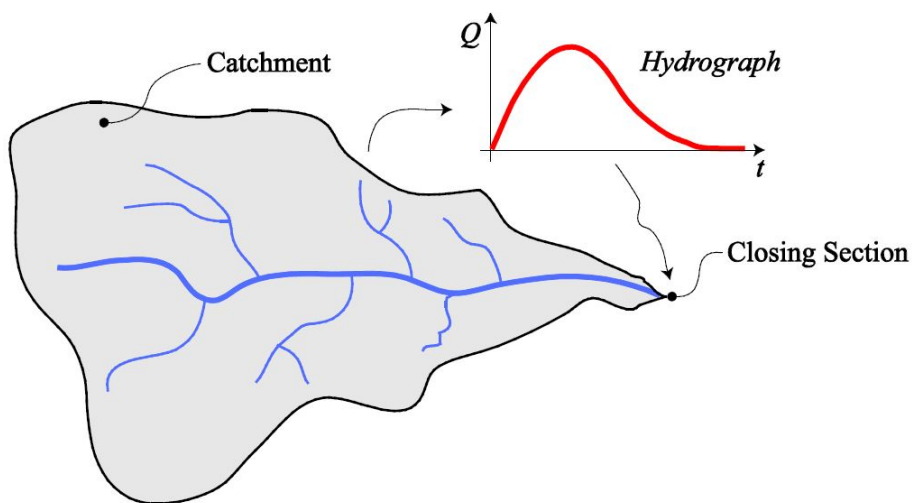


Figure 2.3: The schematic diagram of a hydrographic basin.

A preliminary operation is the catchment area characterization based on the topography of the zone. It refers to the topographical area from which a

watercourse, or a water course section, receives surface water from rainfall (and/or melting snow or ice).

Once the IDF curve has been characterized, a rainfall-runoff method be applied in order to evaluate the hydrograph. This last refers to the flow discharge in the closure section of the catchment as a function of time and constitutes the input for the hydraulic diffusion model (Figure 2. 3). The area under the hydrograph is equal to the total discharge volume for the basin under study. In this procedure is important take in to account the drainage type of the soil.

In a next step, the flood discharge estimated by the hydrograph needs to be propagated through the zone of interest in order to delineate the flood prone areas for various return periods. Flood routing in two dimension is accomplished through the numerical integration of the equations of motion and continuity (dynamic wave momentum equation) for the flow. For this operation may be used the commercial software *FLO-2D®* which is a flood volume conservation model based on general constitutive fluid equations of continuity and flood dynamics. Such two-dimensional flood simulation is based on a digital elevation model (*DEM*) overlaid with the surface grid, areal photography and orthographic photos, detailed topographic maps and digitalized mapping. Such a detailed cartography is needed in order to identify the surface attributes of the grid system; for example, streets, buildings, bridges, culverts, or other flood routing or storage structures. The principal advantages in using a two-dimensional diffusion model is that it can be applied in special cases such as, unconfined or tributary flow, very flat topography and spit flow.

The two-dimensional flood routing for a given surface grid in the flood prone areas, provides the value of maximum water height and velocity for all the nodes within a lattice covering zone of interest, for a given return periods. These results, referred to as the *inundation profiles*, can be visualized as the maximum flood height/velocity maps for a range of return periods. Alternatively, it is possible to represent the results in terms of the flood hazard curves depicting the mean annual rate (or annual probability) of exceeding various flood height/velocities for each node within the zone. In particular, the flood hazard curves in terms of water height denoted by $\lambda(h_f)$, represents the mean annual rate of exceeding (equal to the inverse of return period for a

Methodology

homogeneous Poisson process) of a given maximum flooding height h_f at a given point in the considered area (e.g., centroid of a given building).

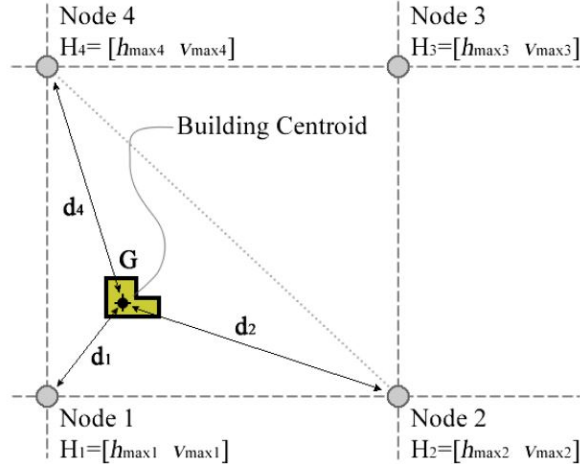


Figure 2.4: Graphical representation of the spatial interpolation for point G.

The hazard curves for a point within the zone of interest (identified as G in Figure 2.4) are extracted from the inundation profiles by performing a spatial interpolation between the flood height/velocity values at the nearby vertices (nodes) of the lattice grid containing the point in question. The flooding height and velocity vector denoted by $\mathbf{H}=[h_{max},v_{max}]$ at a given point can be evaluated as follows:

$$\mathbf{H}_G = \frac{\frac{\mathbf{H}_1}{d_1} + \frac{\mathbf{H}_2}{d_2} + \frac{\mathbf{H}_4}{d_4}}{\frac{1}{d_1} + \frac{1}{d_2} + \frac{1}{d_4}} \quad (2.4)$$

where d_i denotes the distance to node i and \mathbf{H}_i represents the flooding height and velocity vector for node i respectively at a given return period. It can be observed in Eq. (2.4), that the flood height and velocity vector \mathbf{H}_G is calculated as the spatial weighted average of \mathbf{H}_i ; where the weights are equal to the inverse of distance d_i . It is worth noting that only the three closest nodes are taken into account in this spatial interpolation.

Flood may be used as an intermediate variable (i.e., a measure of the intensity of the flood) linking the hydrographic basin analysis and flooding vulnerability assessment of a portfolio of buildings. It should be noted that one could have also used the vector consisting of the maximum flood height and flood velocity pairs as a link between flooding hazard and structural

vulnerability. However, for the sake of tractability of calculations, it has been chosen to use the flooding height as the only interface variable. The flooding velocity for each point in the grid is then calculated from a power-law relation as a function of the flooding height. This power-low relation is characterized for each node within the lattice separately based on the result of flood propagation for the velocity/height pairs for various return periods. In particular, an analytical power-low relation of the form:

$$h_{max} = a \cdot v_{max}^b \quad (2.5)$$

is fitted by employing a linear regression in logarithmic scale for $H=[h_{max}, v_{max}]$ pairs, for all the return period considered.

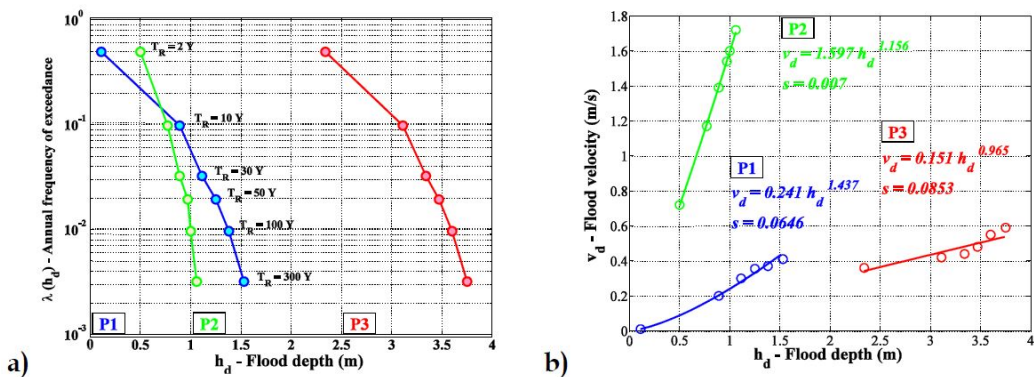


Figure 2.5: a) Hazard curves; b) Flood height versus flood velocity power-law relation.

Figure 2.5 demonstrates three different power-low fits performed for three different points within a given case study area (Suna, Dar es Salaam City).

2.1.3 CHARACTERIZATION OF UNCERTAINTIES AND LOGIC-TREES APPROACH

The uncertainties in a vulnerability assessment problem can be synthetized in the two following sources:

- *In-complete information.* For example some information are missing because in some cases a little part of building (subject to laboratory test) is not representative of the property of the entire building; otherwise property of materials during a test are invalidate due to the elongated contact with water.

Methodology

- *Building-to-building variability.* The fragility curve for a specific structural class is needs to reflect the building-to-building variability in construction buildings within the portfolio.

To evaluate the fragility curves it is necessary to take into account the set of uncertain parameters. The latter have to reflect the building-to-building variability within the class, the loading and the mechanical material properties uncertainties. The uncertain parameters may be enclosed in a vector, named θ that can be subdivided in two categories: *discrete binary uncertain variables* (uncertain logical statements) and *continuous uncertain variables*.

Table 2. 1 reports the list of discrete binary uncertain variables/logic statements considered in the procedure.

Presence of raised-foundation / Platform	<i>PL</i>
Presence of barrier	<i>Ba</i>
Are the doors sufficiently waterproof	<i>DS</i>
Are the windows sufficiently waterproof	<i>WS</i>
Is there a door in the wall panel	<i>D</i>
Are there windows in the wall panel	<i>W</i>
Are there signs of material degradation	<i>DG</i>
Does water born debris hit the structure	<i>DI</i>

Table 2. 1: Discrete binary uncertain variables considered in the procedure.

The continuous uncertain variables considered in the procedure can be classified in three categories: (I) parameters related to building geometry (Table 2. 2 left); (II) parameters related to the mechanical material properties (Table 2. 2 right); (III) parameters related to the structural loading.

<i>L</i> – wall length	<i>f_m</i> – compression strength
<i>H</i> – wall height	<i>τ₀</i> – shear strength
<i>t</i> – wall thickness	<i>f_f</i> – flexural strength
<i>L_w</i> – windows length	<i>E</i> – linear elastic modulus
<i>H_w</i> – windows height	<i>G</i> – shear elastic modulus
<i>H_{wfb}</i> – windows rise	<i>γ</i> – self weight
<i>L_d</i> – door length	
<i>C_d</i> – corner length	
<i>H_f</i> – foundation rise	
<i>H_b</i> – barrier height	

Table 2. 2 - The continuous uncertain parameters: building geometry (left); material mechanical properties (right).

The third category of uncertain parameters considered is the uncertain loading parameters. In particular, the spatial variability of the parameters a and b related to the hydrodynamic flood loading profile have been considered. These parameters describe the flooding velocity as a power-law function ($a \cdot h^b$) of flooding height at a given point, as explained at paragraph 2.1.2). Herein, the parameter a is assumed to be fully correlated to b (through the calculated height/velocity pairs). Thus, in order to simulate the pair of parameters (a, b), only parameter b is simulated.

An efficient ad visual method for modelling the joint probability distribution for several discrete uncertain variables represented as logical statements is *logic-tree*. It is composed of *nodes*, *branches* and *paths*. Each node represents a logic statement (e.g., given value of an uncertain parameter). Each branch in a logic-tree represents the degree of belief (conditional probability) for the logic statement in the destination node given all the statements corresponding to the nodes along the path leading to (and including) the node in the origin of the branch.

For example, in Figure 2. 6, the degrees of belief or the conditional probability values are written in grey characters on the corresponding branch (!, reads as *given* or *conditional on*). Each path in a logic-tree is considered of nodes and branch that connect them; where the nodes belong progressively increasing levels within the tree. The degree of belief in a path (or the joint probability for the specific values of the corresponding uncertain parameters) is equal to the product of the probabilistic corresponding to the branches that construct the path. Finally, for any vertical cut to the three, the sum of the degrees of belief for all the paths trimmed by the cut should be equal to unity. That is, the paths trimmed by vertical cuts represent mutually exclusive and collectively exhaustive logic statements.

The operative way to assess the conditional probability/degree of belief for each node of the logic tree, consists in cataloguing of the survey information, following the condition imposed by the path leading to the node in question. The conditional probabilities corresponding to each branch can be constructed by classifying progressively the building survey results based on the logical value (truth value) of each binary statement. This provides the possibility to take into account the correlation between uncertain parameters/logic statements. The input data necessary for a binary uncertain parameter/logic

statement denoted as BV is the number r of surveyed buildings for which the logic statement is TRUE out of number n of all the building surveyed. Therefore, the probability π that BV is true can be calculated as a complete Beta-function [XI]:

$$p(\pi|r, n) = \frac{(n+1)!}{r!(n-r)!} \pi^r (1-\pi)^{n-r} \quad (2.6)$$

where $p(\pi|r, n)$ denotes the probability distribution for the degree of belief in statement BV given r “success” out of a total of n . The probability π can be estimated in three different ways: (a) the expected value $(r+1)/(n+2)$, (b) the maximum likelihood r/n , (c) sampling from the full probability distribution.

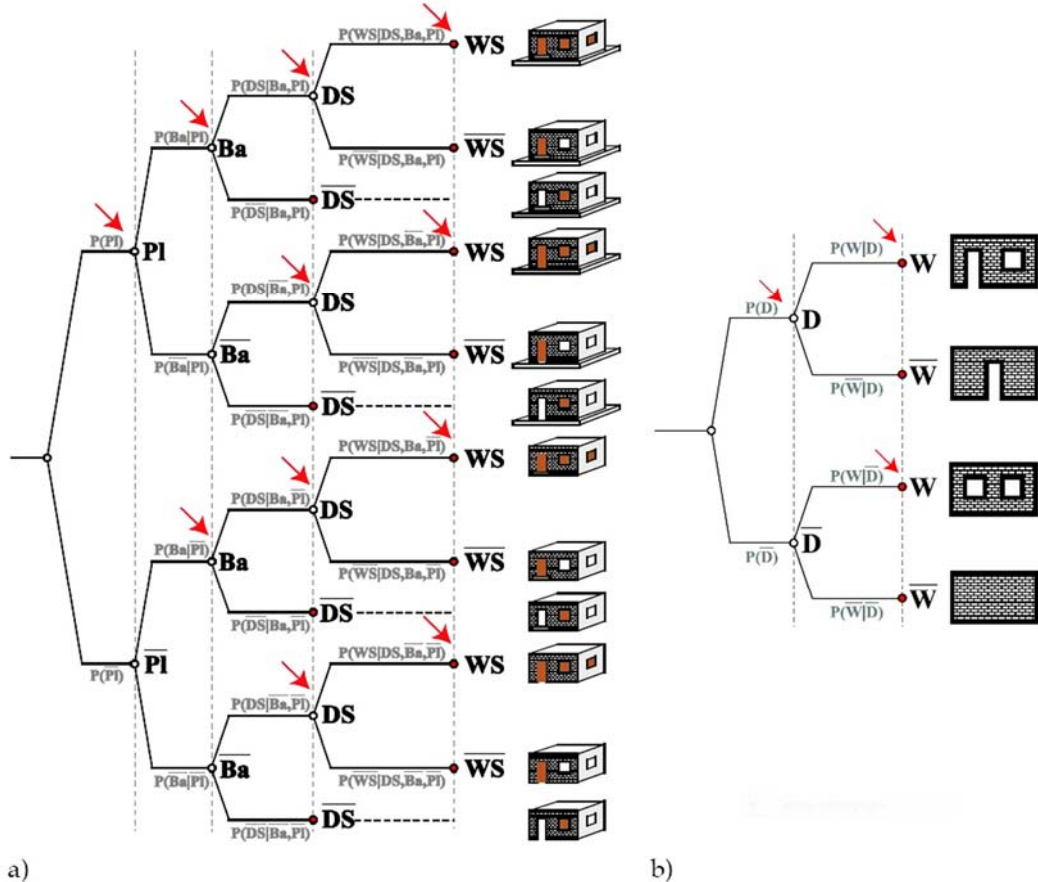


Figure 2.6: a) logic tree for the waterproofness, b) logic tree for the model generation.

2.2 Vulnerability and risk assessment

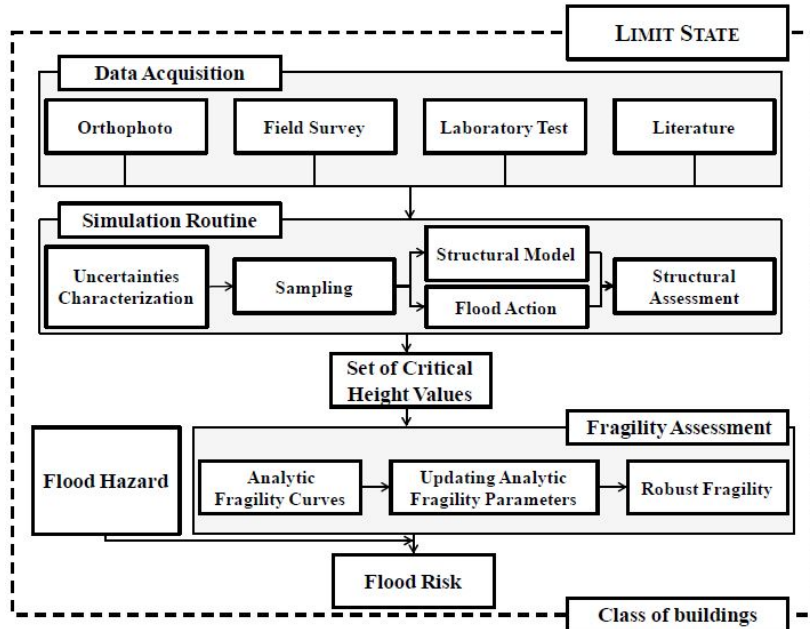


Figure 2.7: Procedure used to vulnerability assessment.

The vulnerability assessment results are represented as the fragility curves, expressing the probability of exceeding a prescribed limit state. To arrive to these results it is necessary to go through a list of consequential operation that, starting with the input data acquiring, leads to realize a mathematical model that allow to resolve the vulnerability assessment problem.

Figure 2.7 represents a schematic diagram of the procedure used for the assessment of the vulnerability of the portfolio of structures. In the paragraph 2.1 are been characterized the input data sets that describes the problem. In this paragraph it is explained how the structural model and action model are generated from the input data.

2.2.1 LIMIT STATES DEFINITION

The definition of limit states, in this methodology, is obtained in order to describe the possible limit situation that the flooding problems may causes. The limit states considered are three and are named: *serviceability (SE)*, *life safety (LS)*, *structural collapse (CO)*. One of the three limit states is considered reached when the corresponding critical water height threshold is passed. This choice is

coherent with the variable *water-height* chosen as scalar variable for the integration of flooding hazard and vulnerability.

Below are shortly described the mean of the three limit states considered for the application of this methodology.

Serviceability (SE). This limit state is reached when the flood height is such that the normal activities in a building are interrupted. In a building the activities are interrupted when the water enter inside therefore the critical water height for this limit state depend by the waterproof capacity of the closure systems (doors and windows). The critical height corresponding to SE limit state can assumes the same value of one of other limit states because if (for example) a building is realized according to flood-resistant criteria, the critical water height related to serviceability can be as large as the critical height needed for exceeding the life safety or collapse limit state.

Life Safety (LS). This limit state is reached when the lives of the inhabitants of the buildings is going to be in danger. This situation may be caused by two reason: (I) water inside building reach a level that puts at risk people life; (II) people life is at risk because water produces the structural collapse. For these reasons LS is a hybrid limit state because its definition is related to both structural/non-structural elements damage and also the exposure of the people inside at the life risk. The critical height of LS limit state is obtained as the minimum value between a water-height quantified with a structural analysis and a nominal water-height that represent the critical flood height (established based on the expert judgment or literature, for example [I]) considered dangerous for the people life.

Collapse (CO). This limit state is reached when a building (or a part of it) loses its bearing capacity. For example flood may produce: collapse of walls, loss of support of the roof, loss of loading bearing capacity due to elongate contact with water or salinization. The value of critical flood height that represent CO limit state evaluated through structural analysis.

2.2.2 FLOOD ACTION

Actions of flooding may be divided in three different load kinds on the structural elements. These are: load of the hydrostatic pressure; load of hydrodynamic pressure (eventual); accidental action induced by the impact of waterborne debris (eventual).

The **hydrostatic pressure** is governed by the follow Stevin's law:

$$p_{hs}(z) = \gamma_w \cdot (H - z) \quad (2.7)$$

where γ_w is the specific weight of water, z is the abscissa measured from the bottom of the structure and H is the flooding height.

The **hydrodynamic actions** can be induced to both flow velocity and transient water level. This last effect is unimportant in an urban context so that the force induced by a water flow with velocity v and flow discharge Q can be evaluated as:

$$S_{hd}(z) = C_d \cdot \rho_w \cdot Q \cdot v \quad (2.8)$$

where C_d is the drag coefficient (typically ranges between 1.2 and 2.0 according to [II]) and ρ_w is the mass density of the water ($\rho_w = \gamma_w/g$ with g gravity acceleration). Thus, the hydrodynamic pressure at height z from the ground can be derived as:

$$p_{hd}(z) = C_d \cdot \rho_w \cdot v^2(z) \quad (2.9)$$

Consequently the hydrodynamic pressure distribution is directly related to the velocity profile along the height. In lieu of detailed hydraulic calculation, the distribution of velocity along the height can be obtained based on simplified assumptions. With reference to Figure 2.8 an approximate velocity profile may consists in adopting a parabolic profile that reaches the maximum velocity at the flow surface with a vertical slope. This assumption allow to write the velocity profile as follow:

$$\frac{v(z)}{v_{max}} = -\left(\frac{z}{h}\right)^2 + 2 \cdot \left(\frac{z}{h}\right) \quad (2.10)$$

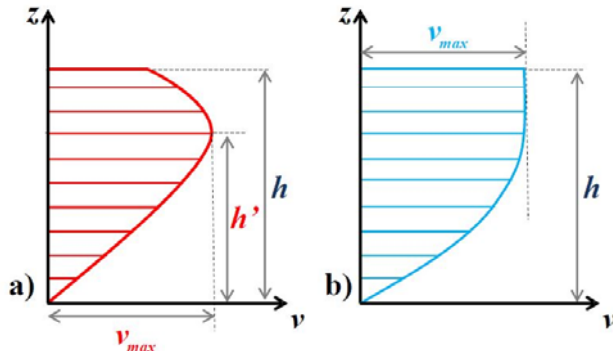
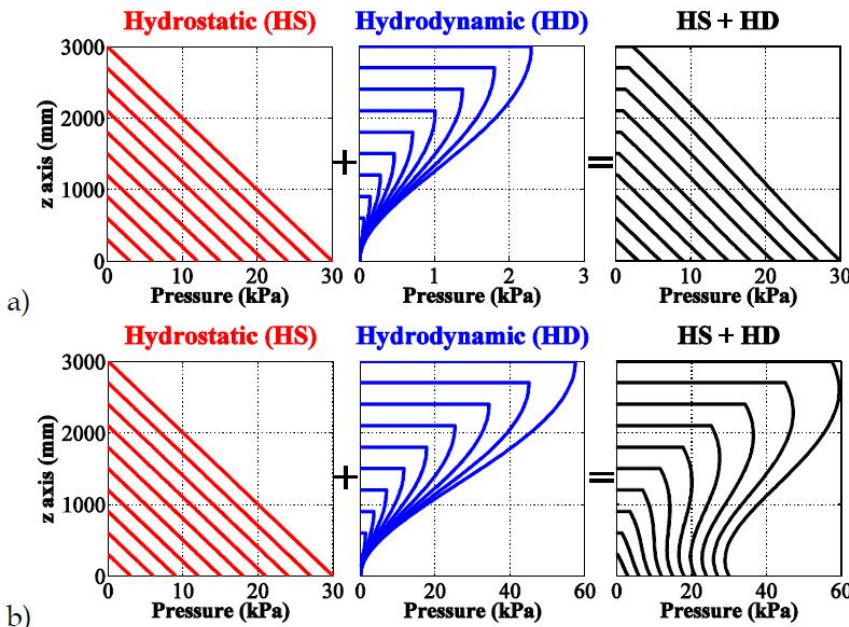


Figure 2.8: a) real velocity profile; b) approximate velocity profile.

The **flood pressure profile** is calculated as the sum of the hydrostatic and hydrodynamic pressure profiles. Figure 2. 9 illustrates the total pressure acting on the wall panel of two alternative combinations of the parameters a and b (that describe the power law (2. 5)). The values are respectively (0.3, 1.15) and (1.5, 1.15) and represent two points with low flood velocity and height and high flood velocity and low flooding height respectively. The contribution of hydrodynamic pressure is significant in the case of with small flooding height and large flooding velocity. Generally the hydrodynamic contribution can be more significant for flood velocity values larger than 1 m/s.



*Figure 2. 9: Hydrostatic and hydrodynamic pressure profile for two different pairs of parameters:
(a) low flooding height and low velocity; (b) low flooding height and high velocity.*

When velocity profile is known, it is possible to evaluate the **accidental debris impact** for example with the approach outlined in FEMA 1995 through the following relation:

$$F_{DI} = \frac{W_D \cdot v_D}{g \cdot t} \quad (2. 11)$$

where W_D is the debris weight; v_D is the debris velocity assumed that the debris is waterborne, ($v_D=v_{max}$); g is the gravity acceleration; t is the impact duration. In this methodology the debris impact position is randomized and if it corresponding to a door or a windows, the load induced by the impact, is translated to the boundaries of the opening.

2.2.3 THE STRUCTURAL MODELLING

The methodology explained in this chapter employs an elastic finite element model (FEM) in open-source software OpenSees. Employing FEM provides the possibility of modelling the real geometry of the structure, taking into account the openings (doors and windows) and irregularities.

The model consisted of two-dimensional elastic shell finite elements panels with openings considered as void. Are considered three type of transversal boundary condition restraints: (a) fixed end; (b) hinged; (c) free.

In order to take into account the uncertain parameters related to the geometrical configuration of the buildings, four different models are generated, which distinguished on the type, number and relative position of the openings in the wall. Figure 2. 10 shows the different models of wall where the number and the position of openings is randomized.

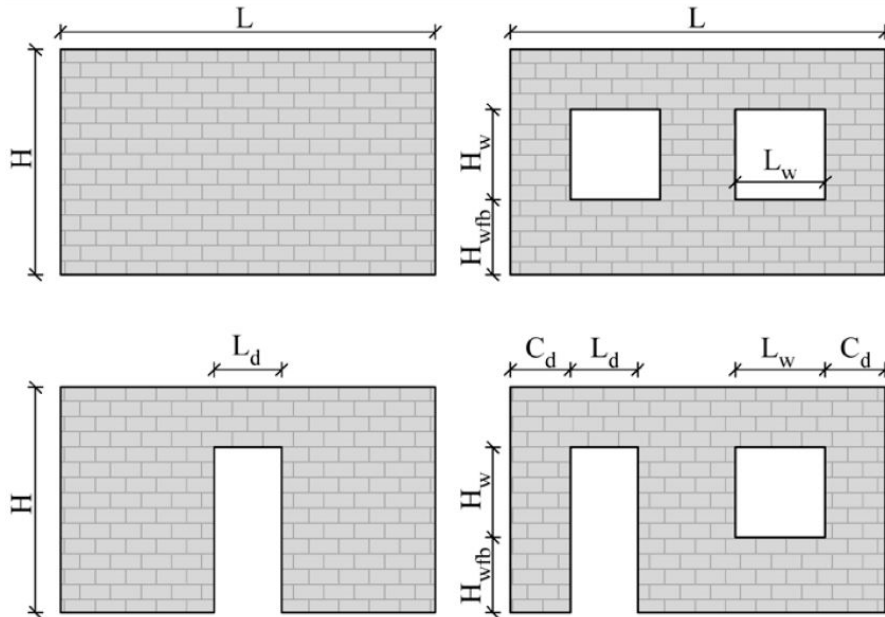


Figure 2. 10: Various models of wall

In the panel are identified various zones sensible at the stress caused by the flooding in terms of shear and out-of-plane bending moment. Denoting the flexural strength of a horizontal section by ($M_{Rd,H}$); the flexural strength of a vertical section by ($M_{Rd,V}$); the shear strength by (V_{Rd}) it has:

$$M_{Rd,H} = \frac{N \cdot t}{2} \cdot \left(1 - \frac{N}{0.85 \cdot f_m \cdot A} \right) \quad (2.12)$$

Methodology

$$M_{Rd,V} = \frac{f_{ft} \cdot H \cdot t^2}{6} \quad (2.13)$$

$$V_{Rd} = A \cdot \tau_0 \quad (2.14)$$

where A is the area of section; H is the height of the section; N is the axial force acting on the section. The formula for shear strength neglects interactions between shear/axial forces. The flexural strength for a horizontal section in Eq. (2. 12) is calculated assuming that the bending moment strength is reached by exceeding the ultimate compression strength. The flexural strength for a vertical section in Eq. (2. 13) is calculated by assuming that the out-of-plane bending moment strength is reached by exceeding the ultimate tensile strength.

The structural assessment for each (increasing) flooding height considered, consist of checking whether the section demand D exceeds the corresponding section capacity C (in terms of shear and bending moment) for the critical sections. For all the identified zone of stress concentration (highlighted in Figure 2. 11) and for each water height level, safety-checking is performed.

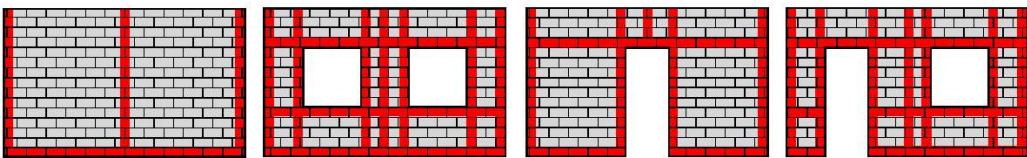


Figure 2. 11: Zones of panel in which is searched the critical section.

For each critical section i considered, the zone(s) of high stress concentration are identified by:

- a) discretizing in smaller *sub-sections* (e.g., with a discretization step of 25 cm);
- b) calculating the demand to capacity ratio (for both flexure and shear), for each sub-section i of the critical section considered, denoted by D_{ij}/C_{ij} . This operation is done in mode of considering all the possible subsection (that have all the possible length and all the possible position along the critical zone);
- c) defining the zone(s) of high stress concentration as those having the largest demand to capacity ratio $\max_j[D_{ij}/C_{ij}]$.

2.2.4 THE STRUCTURAL ANALYSIS

After the definition of the models, the actions, the limit states and the verification criteria, it is possible to explain the analysis routine. The analysis procedure is an efficient simulation-based-procedure realized on a variable number of Monte Carlo simulations (20-50 simulations are generally sufficient). The simulation are based on the extraction of the uncertain parameters in order to have a model of wall on which apply the analysis routine with OpenSees. The output of the simulation, then, is a set of critical height values calculated for various realization of uncertain parameters. Each realization is sufficient to uniquely define the structural model and loading.

Analysis provides a set of critical water height values that corresponding to the reaching of the various limit state considered. Following are explained the criteria with which analysis procedure due to determinate the critical water height for each limit state.

Serviceability. This limit state is reached if the water infiltrate inside the buildings. For this reason, for each structural model and loading identified by the simulation realization, the critical water height corresponding to SE limit state is obtained based on the geometrical configuration and of the water-tightness of the structure (established based on the waterproofness of the closure systems). Figure 2. 12 demonstrates the different values of critical water height assigned based on structural configuration and water-tightness. Filled doors and windows are water-tight. Conversely, white doors and windows are not water-tight.

Structural Collapse. For each simulation realization, the critical flooding height for this limit state is evaluated based on safety-checking in the strategic section identified in Figure 2. 11. If the structure does not reach the collapse limit through the incremental flood analysis, a *sentinel value*¹ is assigned to the critical height. Figure 2. 12 summarizes various situations that may arise for different simulation realizations with the following symbols:

- A. is considered only hydrostatic loading along the height of the structure;
- B. is considered only hydrostatic loading up to the windows level;
- C. is considered only hydrostatic loading up to the height of the barrier;

¹ It is a larger number assigned when the analysis on the structure don't reach the collapse. The analysis is interrupted when the height of water reach the height of the building. This circumstance occurs when the closure system are waterproof and the structure have a good bearing capacity.

- D. is assigned a sentinel value as the critical height;
- E. is considered hydrostatic, hydrodynamic and eventually debris impact actions along the height of structure;
- F. is considered hydrostatic, hydrodynamic and eventually debris impact actions up to the height of windows (for higher elevations the hydrostatic pressure is neglected);
- G. is considered only hydrodynamic and (eventually) debris impact actions along the height of the structure, unloading the openings (since they are not water-tight).

Life Safety. This is an hybrid limit state because the value of critical water height is obtained based on combines of structural collapse evaluations and life safety considerations due to presence of water. Therefore, for each simulation realization, the critical water height is calculated as the more critical between (i.e., the minimum value) critical value calculated for the limit state of collapse and a prescribed nominal value marking a life-dangerous water level inside the building. Figure 2. 12 reports the various situations that may arise during the simulation process.

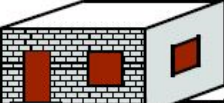
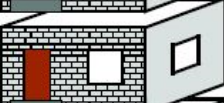
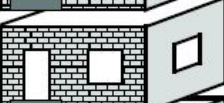
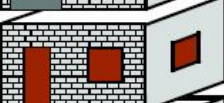
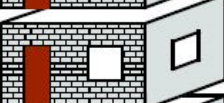
Configuration	Serviceability	Collapse		Life Safety	
		HS	HS+HD	HS	HS+HD
	sentinel value	A	E	$h_{collapse}$	$h_{collapse}$
	$H_{wfb} (+H_f)$	B	F	$min(h_{collapse}, h_{nominal})$	$min(h_{collapse}, h_{nominal})$
	$H_b (+H_f)$	C	G	$min(h_{collapse}, h_{nominal})$	$min(h_{collapse}, h_{nominal})$
	sentinel value	A	E	$h_{collapse}$	$h_{collapse}$
	$H_{wfb} (+H_f)$	B	F	$min(h_{collapse}, h_{nominal})$	$min(h_{collapse}, h_{nominal})$
	$0 (+H_f)$	D	G	$min(h_{collapse}, h_{nominal})$	$min(h_{collapse}, h_{nominal})$

Figure 2. 12: Evaluation of critical flooding height in various situations corresponding to possible Monte Carlo extractions.

The nominal life-threatening water height: This nominal value depends on many factors, namely, presence/absence of flood warning systems, building type, community preparedness, flood risk governance, and demographical aspects (e.g., the children and the elderly are more vulnerable). A recent study [I] demonstrates that, for flooding with rapidly rising water level, flooding height of around 1.5 m corresponds to a 50% mortality rate (i.e., 50% of the exposed people risk their life). In this work, a nominal flooding height value of 1m is chosen that, according to the above-mentioned study, corresponds to a mortality rate of about 10%.

2.2.5 THE ANALYTICAL FRAGILITY CURVES

The simulation procedures until now explained provides, for each limit state, a vector of critical water value. Using these last, through a *Bayesian parameter estimation* [V] it is possible to calculate the posterior probability distribution for the parameters of prescribed analytic fragility functions. In this methodology are adopted three analytical fragility models, one for each limit state defined.

$$(SE) \quad F(h_f | \pi_0, \eta_{SE}, \beta_{SE}) = P(h_{SE} < h_f) = \pi_0 \cdot \Phi\left(\frac{\ln\left(\frac{h_f}{\eta_{SE}}\right)}{\beta_{SE}}\right) + (1 - \pi_0) \cdot I_0(h_f) \quad (2.15)$$

$$(CO) \quad F(h_f | \eta_{CO}, \beta_{CO}) = P(h_{CO} < h_f) = \Phi\left(\frac{\ln\left(\frac{h_f}{\eta_{CO}}\right)}{\beta_{CO}}\right) \quad (2.16)$$

$$(LS) \quad F(h_f | \pi, \eta_{LS}, \beta_{LS}) = P(h_{LS} < h_f) = \pi \cdot \Phi\left(\frac{\ln\left(\frac{h_f}{\eta_{LS}}\right)}{\beta_{LS}}\right) + (1 - \pi) \cdot I(h_f) \quad (2.17)$$

where parameters π_0 , η_{SE} and β_{SE} reported after the conditioning sign ($|$) are the parameters that define the analytic probability distribution/fragility function for the serviceability limit state; $(1 - \pi_0)$ is the probability that the serviceability critical height is equal to zero; η_{SE} and β_{SE} are median and logarithmic standard deviation for the critical water height given that the critical water height is greater than zero for (SE). Meanwhile, for the collapse (CO) limit state, only two parameters denoted by η_{CO} and β_{CO} are defined as the median and logarithmic

standard deviation for the critical water height, respectively. $(1-\pi)$ is the probability that the life safety (LS) critical water height is equal to a nominal prescribed value; η_{LS} and β_{LS} are respectively the median and the logarithmic standard deviation for the critical water height given that the critical water height is assigned nominally; $\Phi(\cdot)$ denotes the standard Gaussian (Normal) cumulative probability distribution and $I_0(h_f)$ and $I(h_f)$ are index functions defined as follow:

$$(SE) \quad I_0(h_f) = \begin{cases} 0 & \text{if } h_f = 0 \\ 1 & \text{if } h_f > 0 \end{cases} \quad (2.18)$$

$$(LS) \quad I_0(h_f) = \begin{cases} 0 & \text{if } h_f \leq h_{nominal(LS)} \\ 1 & \text{if } h_f > h_{nominal(LS)} \end{cases} \quad (2.19)$$

where $I_0(h_f)$ and $I(h_f)$ depict two step functions identified respectively by zero (Figure 2. 13a) and the nominal water height (Figure 2. 13d).

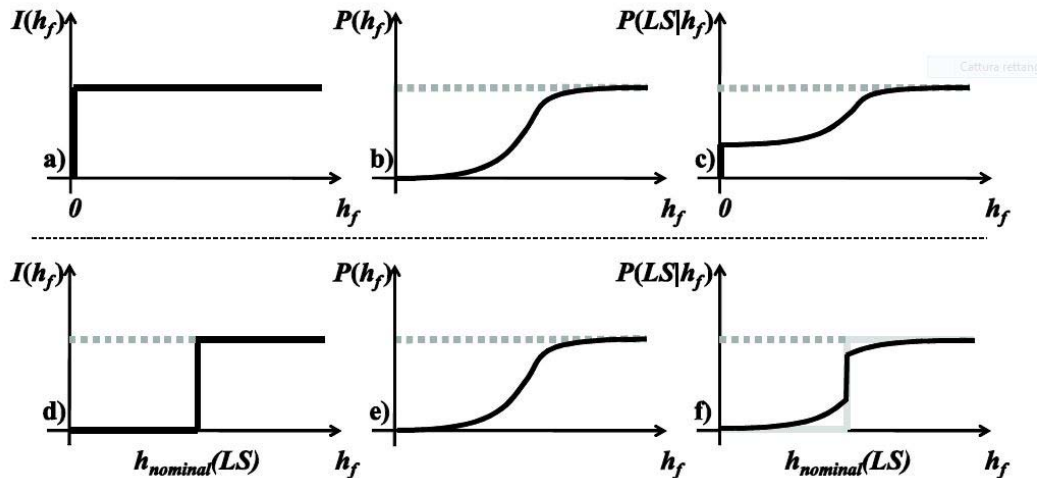


Figure 2. 13 - schematic diagram of: a) step function for SE; b) lognormal CDF for SE; c) three-parameters CDF for SE; d) step function for LS; e) lognormal CDF for LS; f) three-parameters CDF for LS.

The model of analytically fragility defined in Eq. (2. 15) and Eq. (2. 17) may be interpreted as a result of the total probability theorem [VI] on the two mutually exclusive outcomes marked by probabilities π_0 and π . These equations are also known as the *three-parameter* distributions ([VI], [VII]) which are bi-modal probability density functions (PDF)/cumulative distribution functions (CDF) expressed as a linear combination of a lognormal PDF/CDF and a Dirac delta function/step function. In particular the cumulative distribution function

expressed by Eq. (2. 15) and represented in Figure 2. 13c is a linear combination (with weight π_0) of the step function $I_0(h_f)$ denoted in Figure 2. 13a and the lognormal CDF depicted in Figure 2. 13b. In the same manner the cumulative distribution function expressed by Eq. (2. 17) and represented in Figure 2. 13f is a linear combination (with weight π) of the step function $I(h_f)$ denoted in Figure 2. 13d and the lognormal CDF depicted in Figure 2. 13e.

Considering the parameters of the analytic fragility function as $\chi=[\eta,\beta]$ for the collapse limit state and $\chi=[\pi,\eta,\beta]$ for the others limit states, the joint probability distribution for the vector χ may be denoted as $p(\chi)$. Using formulas described in [V] based on the set of critical height values obtained from simulation, the probability distribution $p(\chi)$ for the parameters of the fragility distribution may be update using a Bayesian updating. The probability distribution updated can be denoted as $p(\chi|H_c)$ in which H_c is the vector of n critical height values². Following is described the Bayesian updating procedure used to update the parameters of the *three-parameter* distribution used for SE and LS limit states. The updating of *bi-parameter* distribution for CO limit state can be considered as a particular case of the previous procedure.

The probability $p(\chi|H_c)$ can be written (assuming independence between the pair (η,β) and π) as:

$$p(\chi|H_c) = p(\eta,\beta|H_c) \cdot p(\pi|H_c) \quad (2. 20)$$

where $p(\eta,\beta|H_c)$ represent the joint probability density distribution for parameters η and β given the vector of critical water height H_c , and can be written as [V]:

$$p(\eta,\beta|H_c) = k \beta_{H_c}^{-(n+1)} \cdot \exp \left[-\frac{vs^2 + n(\log(\eta_{H_c}) - \overline{\log(H_c)})^2}{2\beta_{H_c}^2} \right] \quad (2. 21)$$

where k is a normalization factor; n is the number of simulations; $v=n-1$ is the degree of freedom; $\overline{\log(H_c)}$ is the sample average for $\log(H_c)$, and vs^2 is sum of the squares of the residuals calculated based on the sample average value.

Finally the term $p(\pi|H_c)$ can be evaluated from the complete-Beta function represented in Eq. (2. 6), replacing n by the number of simulations and r by the number of simulations in which the critical height values in not assigned nominally.

² n is the number of the simulations executed in the analysis phase.

2.2.6 THE ROBUST FRAGILITY ESTIMATION

At this stage it is possible to construct an analytical probability model based on the set of critical water height values but, in consideration of the many sources of uncertainty present in the vulnerability assessment problem, it is desirable to establishing a *confidence interval*. This last is function of the number of simulations and is evaluated as an interval around the expected value of plausible analytic fragility curves delimited by a plus/minus one standard deviation. This kind of fragility model is called *robust fragility curve* ([VIII], [IX]).

The robust fragility curve is evaluated as the expected value of analytic function $F(h_f|\chi)$ in equations (2. 15), (2. 16) and (2. 17) over the entire domain of vector χ and according to the updated joint probability distribution $p(\chi|H_c)$:

$$F(h_f|H_c) = E[F(h_f|\chi)] = \int_{\Omega} F(h_f|\chi) \cdot p(\chi|H_c) \cdot d\chi \quad (2. 22)$$

where $E[.]$ is the expected value operator and Ω is the domain of the vector χ . The variance σ^2 in fragility estimation can be calculated as:

$$\sigma^2[F(h_f|\chi)] = E[F(h_f|\chi)^2] - E[F(h_f|\chi)]^2 \quad (2. 23)$$

where $E[F(h_f|\chi)]^2$ can be calculated from Eq.(2. 22) replacing $F(h_f|\chi)$ with $F(h_f|\chi)^2$.

Monte Carlo simulations can also be used for calculating the robust fragility from integral in Eq. (2. 22). This method consist of generating N various realizations of vector χ based on the posterior probability distribution $p(\chi|H_c)$. This operation leads to generate N plausible fragility curves. For these curves it is possible to calculate all statistics (e.g., mean, standard deviation and various percentiles) in particular the 16th, 50th and 84th percentile fragility curves can be obtained and this three percentiles, hereafter, are going to be referred to as the *robust fragility curves*.

Assuming independence between the pair (η, β) and π , the simulation of χ based in its probability distribution $p(\chi|H_c)$, implicates separate simulation of (η, β) and π . In order to simulate the pair (η, β) according of its distribution $p(\eta, \beta|H_c)$, β is first simulated from its marginal distribution $p(\beta|H_c)$:

$$p(\beta|H_c) = k' \beta_{H_c}^{-(v+1)} \cdot \exp\left[-\frac{vs^2}{2\beta_{H_c}^2}\right] \quad (2. 24)$$

Conditioning on the simulated value β , η is then simulated based on the conditional probability density function $p(\eta|\beta, H_c)$:

$$p(\eta|\beta, \mathbf{H}_c) = \frac{1}{\eta} \cdot \left(\frac{2\pi \cdot \beta_{H_c}^2}{n} \right)^{-0.5} \cdot \exp \left[-\frac{n}{2\beta_{H_c}^2} \cdot (\log(\eta_{H_c}) - \overline{\log(H_c)})^2 \right] \quad (2.25)$$

As mentioned above, π can be simulated from the marginal distribution described in Eq. (2. 6).

2.2.7 RISK ASSESSMENT

Micro-scale flood risk assessment may be easily expressed in the equation (2. 26):

$$\lambda_{LS} = \int_{h_f} P(LS|h_f) \cdot |d\lambda(h_f)| \cdot dh_f \quad (2.26)$$

where λ_{LS} denotes the risk expressed as mean annual rate of exceedance of a given limit state (LS). The limit state refers to a threshold (in terms of critical water height or critical water velocity) for a building.

The mean annual rate of exceeding the limit state λ_{LS} is later transformed into the annual probability of exceeding the limit state assuming a homogeneous Poisson process as a model for occurrence of limit state-inducing events.

The equation (2. 26) divide the flood risk assessment procedure in two main modules, namely, the hazard assessment module which leads the calculation of the mean annual frequency $\lambda(h_f)$ of exceeding a given flooding height h_f and the vulnerability assessment module which leads to the calculation of the flooding fragility curve in terms of the probability of exceeding a specified limit state $P(LS| h_f)$.

The annual probability of exceeding a limit state $P(LS)$, assuming a homogeneous Poisson process model with rate λ_{LS} , can be evaluate as:

$$P(LS) = 1 - \exp(-\lambda_{LS}) \quad (2.27)$$

The annual rate of exceeding and the probability of exceeding a given limit state are not sufficient to express the exposure to risk. This last, in facts, may be quantified by calculating the *total expected losses* or the expected *number of people affected* for the portfolio of buildings.

The expected repair/replacement coast (per building or per unit residential area), $E[R]$, can be calculated as a function of the limit state probabilities and by defining the damage state i as the structural state between limit state i and $i+1$:

$$E[R] = \sum_{i=1}^{N_{LS}} [P(LS_{i+1}) - P(LS_i)] \cdot R_i \quad (2.28)$$

where N_{LS} is the number limit state that are used in the problem in order to discretize the structural damage; R_i is the repair/replacement cost corresponding to damage state i ; and $P(LS_{N_{LS}+1})=0$.

The expected number of people affected by flooding can also be estimated as a function of the limit state probabilities from Eq. (2. 28) replacing R_i by the population density (per house or per unit residential area).

Chapter 3

INTRODUCTION TO VISK

VISK is the name of the software presented in thesis, acronym of Visual Vulnerability and (flooding) rISK. It is a GIS-compatible computer platform with a Matlab®-based graphical user interface that performs detailed (micro-scale) flood risk assessment for building stock with more-or-less similar characteristics. The GIS compatibility allows for graphical processing of both input and output to the program, providing an efficient visualization of flooding risk. At the core of the platform lies a comprehensive probability-based algorithm for the assessment of the vulnerability of a class of buildings to flooding. This Bayesian algorithm is based on assigning prescribed analytic uni- and bi-modal probability distributions for characterizing the flooding structural fragility functions. The fragility calculations are performed on a bi-dimensional finite-element structural model considering the openings (door and windows) constructed using open-source software OpenSees. The uncertain structural modelling parameters are characterized through, orthophoto recognition, sample in-situ building survey, laboratory test results for material mechanical properties and literature survey. Finally, the risk map is generated by integrating the flooding hazard and fragility taking into account additional information on the exposure (e.g., repair costs, population density, etc.). The results can be visualized both in a detailed building-to-building scale (of potential interest to single house-holds) or as overall estimates for the entire area (of interest to policy makers).

3.1 Interface description

VISK software platform is based on a graphical user interface with a visual system of insertion, control and interpretation of results. The planning and the programming of VISK interface, from the beginning, have been focused on the visual impact of the entire procedure so that user may has a good experience to use VISK platform.

VISK presents a rectangular form window interface characterized by a series of panels that allow a division between the input data that user have to insert and the output command to show all results of vulnerability and risk assessment. Graphic interface is very intuitive, functional and at the same time contain all that the generic user needs to execute a good risk assessment. VISK's graphic layout was thought to ensure that all the variable that influence the problem are under user's control.

In this paragraph are explained the functionality of all the element that characterize user interface of VISK platform.

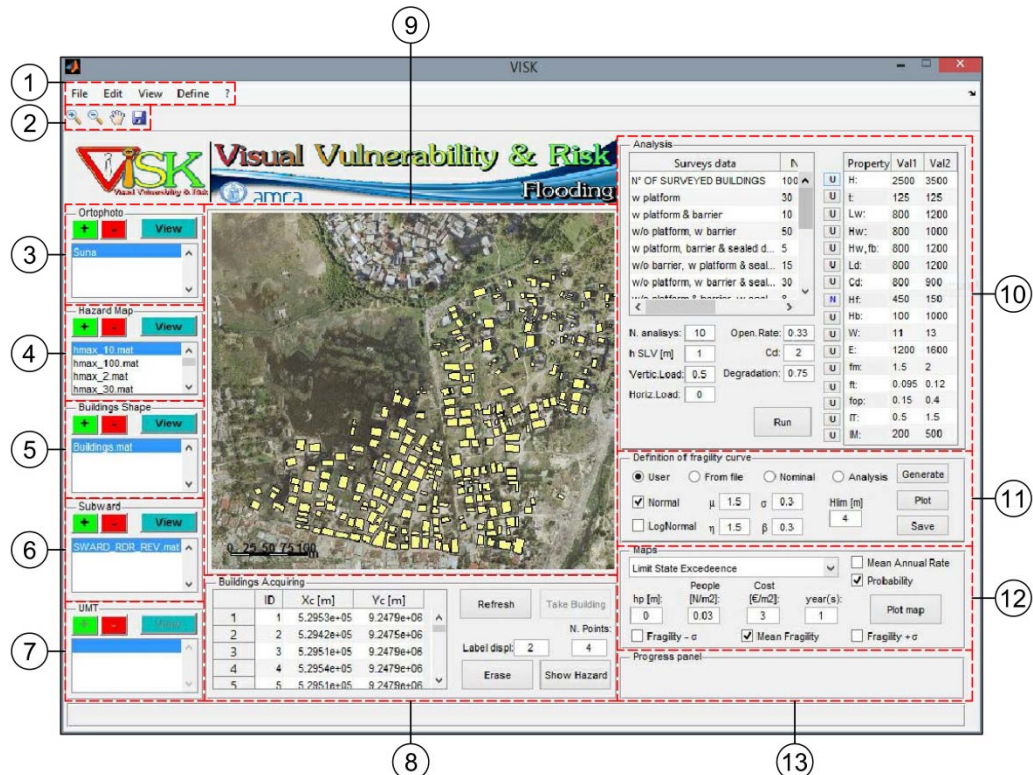


Figure 3. 1: Layout of VISK.

Menu, palette and progress panel.

Main menu of VISK platform [Figure 3. 1 – (1)] is composed of five voices. The menu contain all the function or variables that have not the necessity of a continuous variations or control. The specific function of each voice of menu are now descripted.

- > *File*. In this menu it is possible: to *load* an orthophoto, a hazard map or a buildings shape file; to create a *new buildings shape* file; to open the *interactive database* editor of the building shape file actually in use.

- > *Edit*. In this menu are present the sequent functions: *take actions* to update the data of the shape file in use with the vectors contents the value of the flooding hazards in terms of water height and velocity; *erase all buildings* to clean the shape file of all the data acquired; *enable buildings capture* to activate the graphical class of function designated to the geometrical building acquiring on the map.

- > *View*. This menu enclose: *buildings label* that activate the view of the labels of the buildings acquired; *grid as contour* shows the hazard profile as a contour on the map; *grid as surf* shows the hazard profiles as a surface on the map; *all hazard profiles* plots the diagram of hazard profiles for all the buildings acquired; *hist analysis results* plots an histogram with the frequency of the crisis type observed during the analysis; *analysis report* generates a Microsoft Excel® report of the analysis results; *portfolio analysis* plots the probability that a given percentage of buildings exceeding the given limit state for all the return periods considered.

- > *Define*. In this menu there are the following commands: *limit state* to consider (for the vulnerability assessment) one of the three possible limit states; *extraction options* to choose the function to extract the uncertain parameters (the possibility are: maximum likelihood, expected value, entire distribution); *scale ruler position* to establish the position of the scale ruler on the map shown; *water load* to choose the kind of loading to consider in the analysis (the possibility are: hydrostatic, hydrodynamic, hydrodynamic plus debris impact); *support condition* to assign the condition of the support of the walls in the structural model.

- > ?. In this menu it is possible to open the *help windows* (actually in working) and the *about windows* with the references to the version and the authors.

The *palette of instruments* [Figure 3. 1 – (2)] encloses the function to a good experience in using map viewing. There are in fact the *zoom* and *move buttons* to focalize the view on a specific part of the map and the *save button* to save a particular view of the map in *JPEG* format.

In Figure 3. 1 – (13) is highlighted the panel in which is located a *progress bar* that shows the percentage of conclusion of all the process that VISK elaborates. It is important wait the conclusion of a process before to initialize another to avoid errors and interruptions of the operations.

Orthophoto.

In this panel [Figure 3. 1 – (3)], user has the possibility to insert a high definition picture of the geographic area object of the study. The picture must have two characteristics to be used in VISK: must be in *TIFF* format (*Tagged Image File Format*) and must be accompanied by a *TFW* file that contain GIS information of the map. In particular this file contain six numbers: dimension of a pixel in X direction, two factor of rotation, dimension of a pixel in Y direction, X and Y coordinates of the up-left point of the raster image.

Through loading operation VISK shows on the central panel the map of territory in scale and with all the geographic information.

Hazard map.

Hazard profiles are generated by the execution of and hydraulic computation of the geographic area of interest. This operation, through the knowledge of natural basin, channel where water flow and rainfall data, give (for different return period) the values of height and velocity of flooding expected. These values orderly by return period represent hazard profile of an area in terms of flooding height and velocity. The result of hydraulic computation are extrapolated for a discrete number of points that model a grid on territory of interest. Hazard value are saved in a grid file (with *TXT* extension) that including also geographic information of the points.

Hazard map panel [Figure 3. 1 – (4)] allow to introduce the flood hazard profile related to area object of study. To a correct loading operation of hazard profiles, the name of grid files must be of this type: *hmax_100*. The first letter must be *h* if the profile is related to flooding height or *v* if it is related to flooding velocity. The number, instead, represent the return period of the data

included in the grid file. After the loading operation it is possible to show hazard profiles in two way: user may show it on the map or in a diagram (this last only if the buildings are been already acquired).

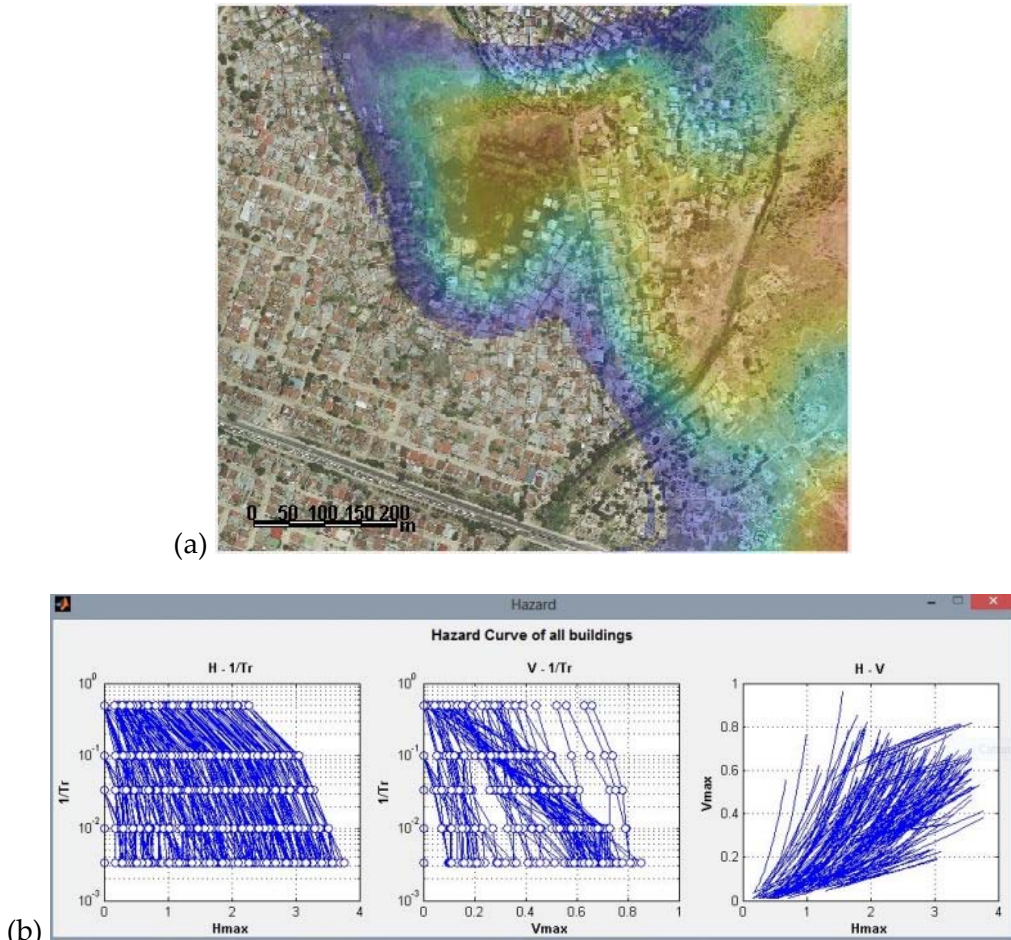


Figure 3.2 – (a): hazard data on the map viewed as surf; (b): hazard curves.

Buildings shape.

The panel related to buildings shape files [Figure 3.1 – (5)], contain two types of file. It may enclose the files created by buildings acquiring operation or generic file created with a generic GIS-compatible program. Both may be showed on the map panel. It is possible to have many building shape files loaded in this panel to confers the possibility to have more workspace simultaneously active.

Subward.

The function of this section [Figure 3. 1 – (6)] is to load and show shape file with boundary information. In reality hear is also possible display all the types of shape file the contain details relate to the map in object such as, rivers, roads, etc.

UMT.

This panel [Figure 3. 1 – (7)] is designated to allow the loading of *UMT* files (Urban Morphology Types). This function is actually in working to extend VISK functionality also in the meso-scale risk assessment.

Buildings acquiring.

In this panel [Figure 3. 1 – (8)] it is possible to capture the buildings on the map that are engaged by the flooding problem. The acquiring operation is very simple, in fact after the definition of the corners number it is sufficient surround building with mouse clicking in corresponding of each vertex. During this graphic procedure, VISK, save geographical information of the building in a the shape file created to receive the portfolio of buildings. For each building acquired, in the table, appear an *identification number* automatically assigned and the *geographical coordinates* of the midpoint of the building. A *refresh button* allows to update the view of the buildings acquired while the *erase button* gives the possibility of delete a wrong acquisition. During or after the operations of buildings acquiring it is possible to load the actions for the already acquired buildings from the menu *Edit -> Take actions*. After this procedure it is possible to show the hazard profile for each building simply clicking at first on *Show Hazard* and after on the building of interest.

Map window.

This windows [Figure 3. 1 – (9)] is used to view the input data in visual manner. In addition to the visualization of the maps, buildings acquired, hazard maps (as contour or as surface) it is possible to view an overlapping of all the visual input data. For example for a focused buildings acquiring operation on the structure subject at flooding problem it is possible activate the view of the geographic map and of the hazards map so that user may consider only the buildings located in the area invested by the problem. Furthermore, map

windows, is also a work-windows for the operations of geometrical buildings acquiring.

Analysis panel.

Analysis panel [Figure 3. 1 – (10)] contains all the variables linked to the management of the entire analysis procedure.

On the left side of the panel are sorted all the choice-variable for the *waterproofness-logic-tree* and the *wall-model-logic-tree* explained at the paragraph 2.1.3 and represented in the Figure 2. 6.

On the right side of the panel are sorted all the uncertain variables related to the geometry of the wall model, the materials and the time and mass of debris to considerate for the impact. In the perspective of a good uncertainties treatment of these parameter for each of which it is possible to choose the kind of distribution that best describes the uncertainties of the parameter. The possible distributions are: *uniform*, *normal* and *log-normal*. In the case of *uniform distribution* (Figure 3. 3c) the parameter inputs consists in the minimum and the maximum value that it may be assume. In the case of *normal distribution* (Figure 3. 3a) the parameter inputs consists in mean (μ) and standard deviation (σ). Instead, in the case of *log-normal distribution* (Figure 3. 3b) the parameter input consist in median (η) and standard deviation (β). It is possible to consider also a *deterministic value* of a parameter using the *uniform distribution* type in which the minimum and the maximum value of the parameters are puts equal.

Figure 3. 3 represents the three types of distribution included in VISK algorithm. The abscissa axes is represent a variable parameter (e.g., the wall length) while the ordinate axes represent the probability with which the parameter presents the corresponding value. The distribution curves must be created so that the area under the curve must be equal to 1.

Other parameters located in the analysis panel are:

- *N.analysis*. Number of simulation that VISK must lead to terminate the analysis.
- *hSLV*. Nominal critical height for Life Safety Limit State (par. 2.2.1).
- *Vertic.Load*. Roof vertical load on the wall.
- *Horiz.Load*. Roof horizontal load on the wall.
- *Open.Rate*. Rate of openings in a wall expressed as openings-number/meters.

- C_d . Drag coefficient (par. 2.2.2).

Degradation. Rate of degradation due to elongate contact water.

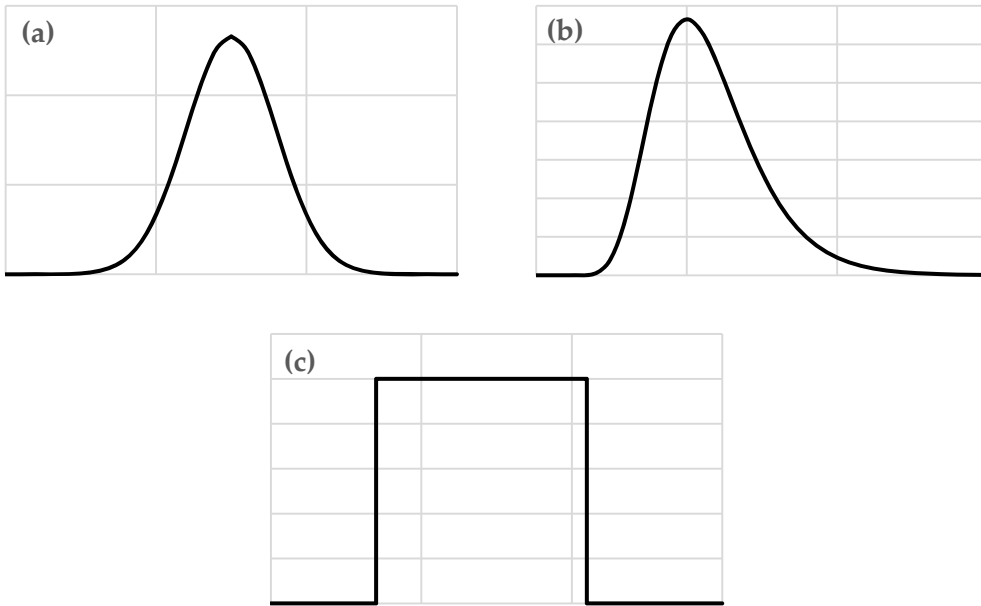


Figure 3.3 - Distribution types: a) normal distribution; b) lognormal distribution; c) uniform distribution.

Definition of fragility curve.

In this panel [Figure 3.1 – (11)] user may define the kind of fragility curve that want to use for risk integration. The possibility are:

- User.* The fragility curve is defined as a normal or lognormal distribution through the input of respectively (μ, σ) or (η, β) .
- From file.* User may load a custom fragility curve from a *txt* file in which abscissas and ordinates are sorted in columns.
- Nominal.* In this case fragility curve is represented by a step function with the step in corresponding of the nominal critical height value of flood insert into analysis panel.
- Analysis.* The fragility curve is evaluated after the analysis procedure as explained at paragraphs 2.2.5 and 2.2.6.

After the selection of the type of fragility curve, this last must be generated through a click on *Generate* button and it may be viewed (using *Plot* button) in a new graphic windows.

Maps panel.

The panel highlighted in Figure 3. 1 – (12) include the functions of risk assessment output in terms of risk maps. The maps that may be plotted are in terms of: *limit state exceedance*, *expected casualties*, *expected financial losses*. All the maps may express the risk in terms of *mean annual rate of exceedance* or in terms of *probability of exceedance* in an established number of years. If the fragility curve is a robust fragility evaluated through the analysis process, all the maps may be plotted as mean value or mean value \pm standard deviation (σ).

3.2 VISK manual

In this paragraph is explained the procedure that leads to a flood risk assessment using VISK-platform.

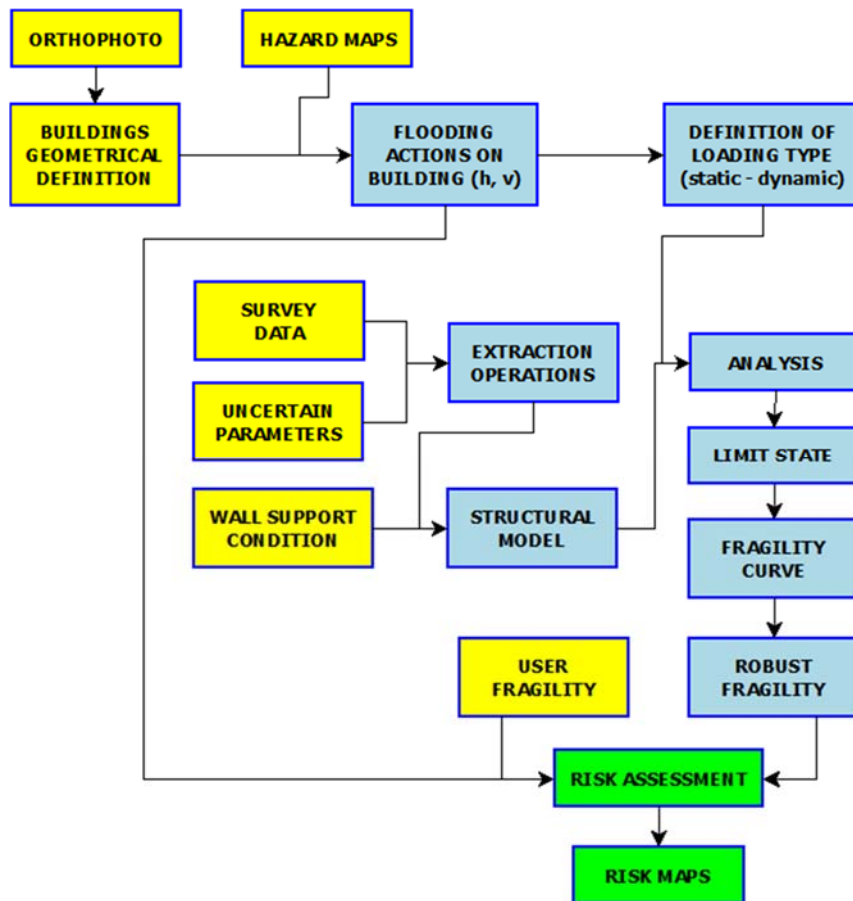


Figure 3. 4: Logic tree of VISK global procedure.

There are two main ways to operate with VISK depending of the kind of fragility curve that user want to use. Fragility curves, in fact, may be both a results of analysis methodology and an input data. The way walk through change substantially the results in terms of risk assessment because a custom fragility curves may not be representative of the real behaviour of the buildings but, otherwise, is not always possible a characterization of the uncertain parameters of the buildings to lead a good analysis so that the unique solution is the using of a literature fragility curves.

Figure 3. 4 represent in a synthetic way the logic tree with which is possible to lead a risk assessment with VISK platform.

3.2.1 WORKSPACE INITIALIZATION

The first operation to accomplish is to load a geo-referred orthophoto of the area in object of study. The quality and the resolution represent and important aspect because all the operation boundaries recognition of the buildings are more accurately as much as high the resolution of the photo. The orthophoto(s) loaded are automatically saved in the workspace so that when VISK is re-opened the orthophoto is automatically showed in the window maps.

When the area of interest is identified it is possible to load the grid files³ of the hazard maps for each return periods. A viewing of the hazard profiles on the maps allow to identify the building invested by the flooding problem. Hazard maps may be showed for one return period at time.

Through the menu *File -> New Buildings Shape* it is possible to create e new file in which to store all buildings data in terms of geometrical position, flooding hazards and (after calculation) risk assessment. Immediately after the creation of a new shape file it is possible the operation of boundaries recognition of the building in the area of interest. For each structure user must insert the number of vertex and must click on *Take Building* button. This operation may take a while, depends of the number of buildings that must be recognized.

³ For each return periods it is necessary to load hazard profiles both in terms of water height and water velocity. If, for example, for a given return period only height hazard profile is loaded, VISK return a series of errors during the take-actions-operation because velocity profile is necessary to fit the power-law $h(v)$. (Ref. Eq. (2. 5)).

Afterwards the buildings boundaries recognition it is possible to update the shape file (containing all buildings data) with the value of flood hazard in terms of height and velocity for all the return periods considered. This is an automatic procedure that can be starts from menu *Edit -> Take Actions*. At conclusion of the procedure it is eventually possible to view a diagram of hazard profiles of all the buildings considered.

In conclusion, the series of operations just described, leads to have a workspace defined on a geographical area with a loading model represented by the hazard profiles and with the geometrical position of the buildings of which is necessary a vulnerability assessment.

3.2.2 BUILDINGS VULNERABILITY ASSESSMENT

The procedure described in this paragraph are necessary only if user wants to evaluate the risk with a fragility curve calculated and not with a custom fragility curve.

The generation of structural models in VISK depend of the uncertain parameters and the waterproofness capacity of the closure systems. To a correctly analysis phase a survey in place is necessary to recognize (for the highest possible number of buildings) the parameters explained at paragraph 2.1.3.

After the definition of the parameters that characterize the mechanical and geometrical models it is possible to start the analysis. This operation may takes also a long time because the number of calculations that VISK must accomplish is very high. The necessary time for the analysis depends of the capacity of the computer on which VISK is working and of the number of simulations that user wants to execute. This last is an important aspect of the analysis results because a very small number (e.g., 10 simulation or less) makes analysis procedure very rapid but the results are more approximately; a very large numbers instead (e.g., 100 simulations or more) gives a good results (in term of approximation) at the cost of a lot of time necessary for the analysis. A good compromise between the time of analysis and an acceptable approximation it has for a number of simulations of about 30-50.

The results of analysis are three vectors (one for each limit state) of length equal to number of simulations. For each limit state, the vector contains the value of water critical height corresponding at the reaching of the considered

limit state. Applying the methodology explained in the paragraphs 2.2.5 and 2.2.6, VISK provides the fragility curve that represent the buildings vulnerability assessment.

3.2.3 RISK ASSESSMENT

When in VISK is defined a fragility curve (analytically calculated or custom made), the program has the possibility to integrate the area under the intersection between the fragility curve and the hazard profile related to a building. This area represent the risk (in terms of limit state exceeding for example) of flooding for the considered building.

To create a risk map, user, must choose in *Maps Panel*: the kind of map that he wants to produce (i.e., *limit state exceedance*, *expected casualties*, or *expected financial losses*) and if he wants the risk value in terms of *mean annual rate* or *probability*. At this point risk assessment procedure is terminated and the map created may be saved as image or it is possible to save risk information, for each buildings, in a shape file.

3.3 VISK structural analysis procedure

The objective of this paragraph is to focus the attention on the specific operations that the VISK platform execute during the structural analysis process. A schematic flowchart that synthetizes the entire procedure is shown in Figure 3. 5.

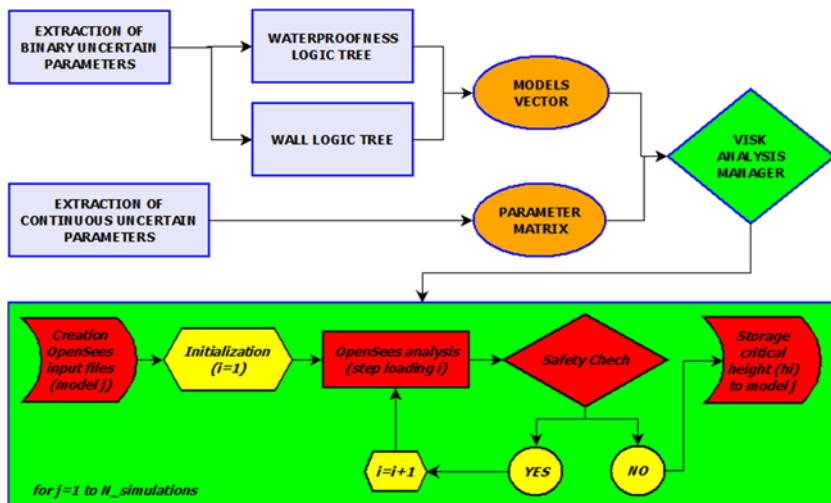


Figure 3. 5: VISK structural analysis flowchart.

When the *Run* button is clicked on VISK interface, a check of all input data is made. A very fast algorithm analyze one at time all the parameters inserted by user to control if all data is defined correctly by user. If data is correct, VISK initiate the structural analysis procedure of the Figure 3. 5.

VISK structural analysis algorithm can be divided in two main steps. In the first step VISK have the purpose to generate the *models vector* and the *parameter matrix*; in the second step analysis be made.

Starting from the uncertain binary parameters, whit the extraction procedure reported at paragraph 2.1.3, VISK builds the logic trees of Figure 2. 6 for a numbers of time equal to the simulations number. In this way VISK creates a *models vector*, that is a vector whose generic element is a number that identify one of the four structural model (Figure 2. 10) correlated at particular waterproofness properties (e.g., the j -th simulation is characterized by a structural model of a wall with door and window and the entire building is waterproof).

Models vector is not sufficient to execute a structural analysis because it is necessary to have the dimensions of the model and the mechanical properties. For these reasons VISK provide to operate another extraction procedure on the uncertain continuous parameters. This process have as result the *parameters matrix*. It is a matrix with number of rows equal to simulations number and number of columns equal to uncertain continuous parameters number. So, a generic row of *parameters matrix* (for example j -th row), represent the characterization of the dimensions and mechanical properties of the j -th model.

Models vector and *parameters matrix* are the two main data inputs of the core of VISK analysis: the *VISK Analysis Manager* (VAM). It is composed by a series of Matlab® scripts and provides to accomplish all the procedures, routines, decisions and checks that allows to have the capacity response of the buildings to the flooding problems. Following are explained the four main tasks of *VISK Analysis Manager*.

Generation of the OpenSees input files. To execute a structural analysis with OpenSees code, it is necessary to define a workspace in which the structural problem is understandable to OpenSees solver. This open source code is programmable in *TCL* code so that the input file of OpenSees must be written in this language. VAM, for this reason, have a procedure that, starting from

models vector and *parameters matrix*, automatically generate the *tcl* files of: nodes, elements, restraints, material, loadings, etc.

Execution OpenSees analysis. When the input files are generated, VAM, manage the analysis procedure with OpenSees code. The analysis have the purpose to establish the bearing flooding capacity of structure whit a linear incremental step-by-step procedure. The analysis step showed in Figure 3. 5 is related only to one step of loading because is the *safety check procedure* that establish if the analysis may be continue or not to a major step of loading. Every analysis result of OpenSees elaboration are saved in a series of *tcl* output file.

Safety check. For each step of analysis a safety control is executed along the critical zones highlighted in Figure 2. 11. The safety control are made in terms of demand/capacity for flexural moment and shear mechanisms. If the check is positive (that is $D/C \leq 1$), the algorithm return on the analysis procedure with an incremented load; instead if the check is negative the algorithm go on the storage procedures.

To realize a safety check, VAM must read the *tcl* output files saved by OpenSees solver and elaborates the data. This operation consist in an integration of the stress saved for each node of the shells (in which the wall is modelled) to have the values of flexural moment and shear along the areas object of verify. These areas are situated along the critical zones and have variable position and extension. VAM, through a reiterative procedure, searches the extension and the position of safety-check-area along the various critical zone that maximize the ratio D/C .

Storage operations. After VAM has individuate the critical height of water for each limit state, it store this data in a *results vector* (clearly defined for each limit state). In add VAM, saves also for each simulation the critical zone where the failure arise and the input data of the model analysed.

3.4 VISK vulnerability and risk assessment

3.4.1 ROBUST FRAGILITY CURVE

The procedure with which VISK elaborate the fragility curves starting from the analysis results, is exhaustively explained at paragraphs 2.2.5 and 2.2.6.

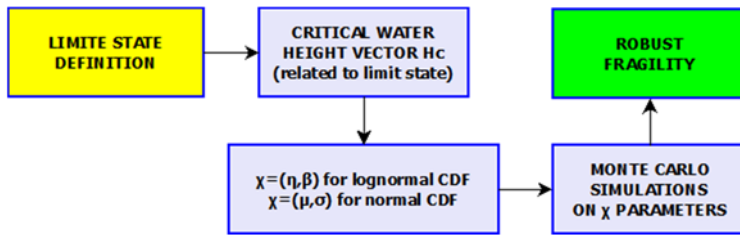


Figure 3. 6: VISK fragility evaluation procedure.

Figure 3. 6 synthesize the global steps that VISK go through to accomplish the evaluation of fragility curve with the confidence interval defined by plus/minus the standard deviation.

VISK Analysis Manager (VAM) manages the analysis routine simultaneously for all the three limit state defined and save the value of critical water height in three different vectors (one for each limit state). At the end of the analysis procedure, to execute a vulnerability buildings assessment, in terms of robust fragility curve, it is necessary to define the limit state respect to which the assessment procedure must be execute. The definition of the limit state is possible through the menu *Define -> Fragility Limit State*.

VISK may evaluate the robust fragility curve both as a normal and a lognormal cumulative distribution of probability in base of the choice that user made into *Definition of fragility curve Panel*.

The fragility calculation procedure in VISK starting with a recognition of all data necessary to the statistics evaluation about the vector of critical water height. For the values of these vector are calculated the pairs of parameters (η, β) in the case of lognormal cumulative distribution of probability or (μ, σ) in the case of normal cumulative distribution of probability. In both cases, following the robust fragility procedure (explained at paragraph 2.2.6), VISK execute on the couple of parameters chosen N Monte Carlo simulations⁴ (one for each realization of the parameters) based on the posterior probability distribution. This operation leads to generate N plausible fragility curves so that it is possible to determinate a confidence interval.

Figure 3. 7 depict an example of a fragility curve plotted by VISK platform. In the picture are visible in grey colour all the plausible fragility curve based on 200 Monte Carlo simulations of the parameters (η, β) of an analysis result

⁴ In VISK is implemented $N=200$.

example. The confidence interval is delimited by the black curves that represent the mean fragility curves plus/minus the standard deviation.

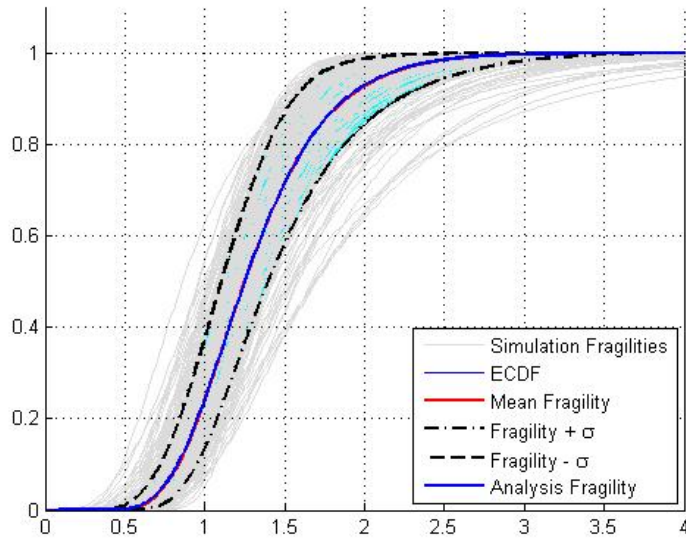


Figure 3.7: Example of VISK robust fragility curve.

3.4.2 OTHERS FRAGILITY CURVE

Another way to use VISK platform is to introduce the buildings vulnerability as an input parameter and not obtaining it through analysis procedure. The possibility of insert a custom fragility curve born by the consideration that is not always possible to have available surveys data, with the consequence that is impossible to characterize the uncertain parameters to realize acceptable structural model. So, in all the cases in which it is impossible to execute a vulnerability assessment it is possible to characterize in VISK platform a custom vulnerability to flooding problems (represented by the fragility curve).

VISK allows the introduction of the four types of custom fragility curves represented in Figure 3.8. On the abscissa axes is returned the height of flooding and on the ordinate axes is returned the probability of exceeding a given height of flooding.

To characterize the normal and lognormal kind of fragility curve (reported in Figure 3.8a and Figure 3.8b) are necessary to define respectively the

parameters (μ , σ) and (η , β). With the definition of these parameters VISK automatically generate the corresponding curve.

Nominal fragility curve is the most simply fragility definition because it confers a totally vulnerability or a nothing vulnerability depending if the flooding height is larger or not of a nominal value.

The last possibility is to load a fragility curve from a *txt* file in which the curve is defined of a discrete number of point.

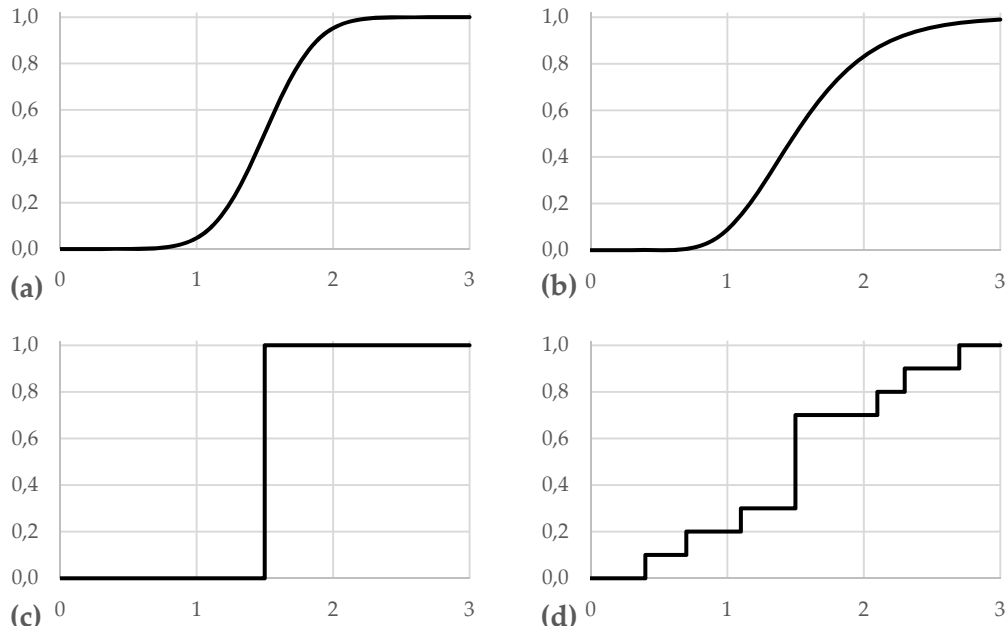


Figure 3.8 - Custom fragility curves: a) normal CDF; b) lognormal CDF; c) nominal step function; d) totally custom fragility curve.

3.4.3 RISK INTEGRATION

After the vulnerability assessment of building produced by the analysis process or after the vulnerability definition through a custom fragility is possible to evaluate the risk.

VISK estimates flooding risk, of a given point, by integrating the fragility curve (robust with its plus/minus one standard deviation interval or custom) and the flood hazard at a given point in the zone of study.

VISK procedure to risk assessment follows the criteria exposed at paragraph

2.2.7.

Chapter 4

CASE STUDY: SUNA

In this Chapter an application of the proposed methodology to risk assessment with VISK platform is leaded. The case study regards Suna, a city in Dar Es Salaam (Tanzania) in which the flooding problem is more important because the city is located near a flood-prone area of the Mizimbazi river.

In this Chapter the entire methodology presented before is applied with VISK platform. Are reported all the input data used to characterize the flooding action (in terms of flooding hazard curves) and the uncertain parameters to define the structural model and the analysis logic tree.

An exhaustive study is leaded to show the effects of: the number of simulations, the extraction criteria used to choose the uncertain parameters, the kind of probability distribution in fragility curve evaluation, the water load typology.

In the end the risk assessment is reported in a visual manner (maps) and in numerical manner as numbers of people that risk their life and financial losses due to flooding problem.

4.1 Hazard flooding definition

4.1.1 THE IDF CURVE: HISTORICAL AND CLIMATE PROJECTIONS DATA

To perform a risk flooding assessment two sets of rain-fall curves are been considered: the first based on historical data (from 1958 to 2010) and the second based on specific climate projection scenario provided up to 2050. Henceforth, historical scenario will be denoted as H and the climate projection scenario will be denoted as CC.

The IDF curves for are obtained as descripted at paragraph 2.1.2 and, the equation (2. 3), are follows specified for the two scenarios:

$$(H) \quad h_r(d, T_R) = K_{T_R} \cdot 36.44 \cdot d^{0.25} \quad (4. 1)$$

$$(CC) \quad h_r(d, T_R) = K_{T_R} \cdot 31.70 \cdot d^{0.26} \quad (4. 2)$$

where the values of growing factors K at the various return period are reported in Table 4. 1:

T_R	2 Ys	10 Ys	30 Ys	50 Ys	100 Ys	300 Ys
H	0.95	1.42	1.70	1.83	2.01	2.29
CC	0.94	1.50	1.84	2.00	2.21	2.41

Table 4. 1: Growing factors for the different return periods (H: historical, CC: climate change).

The historical rainfall data is registered through a meteorological station locate in Dar Es Salaam Airport at 55 meters altitude from sea level, $6^{\circ}86'$ latitude South and $39^{\circ}20'$ longitude East. Through these recordings, the mean annual rainfall for Dar Es Salaam city is estimated around 1110mm.

Figure 4. 1 represent the rainfall curves with and without climate change effects sorted by the six different return periods considered. For Dar Es Salaam city, the climate scenario considered loads to a decreasing of rainfall intensity, visible in the figure because the dotted lines (representative of the climate change scenario) are lower than those continuous lines (representative of the historical rainfall data). Also if the rainfall intensity decrease, considering the climate projections, the growing factor demonstrates a slight increase. It represent a function of the coefficient of variation for the extreme value distribution so that a height value (with constant mean or central value) leads to higher probability for extreme events.

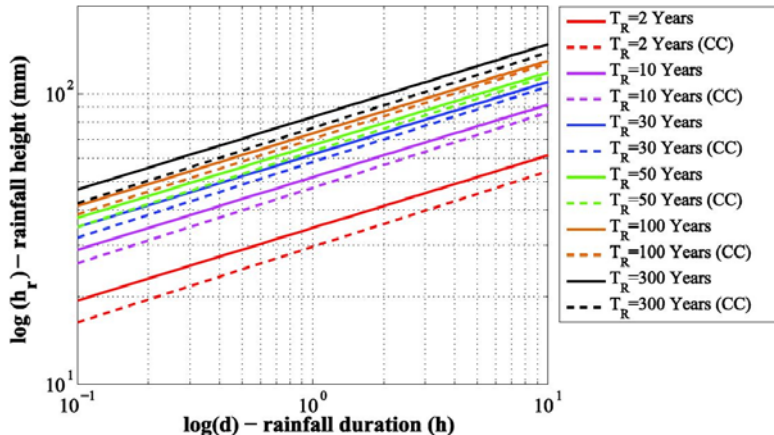


Figure 4. 1: Rainfall Probability curves for DSM city with and without climate change effects.

4.1.2 CATCHMENT AREA AND HYDROGRAPHS DEFINITION

The definition of Mizimbazi river catchment identifies three areas that are shown in Figure 4. 2. In this picture is highlighted also the city of Suna. Catchments are geologically characterized mainly by clay-band sands and gravels (corresponding to soil group B in the Curve Number method). The land use of catchments 1 and 2 are characterized mainly by agricultural use and catchments 3 is characterized as residential area.

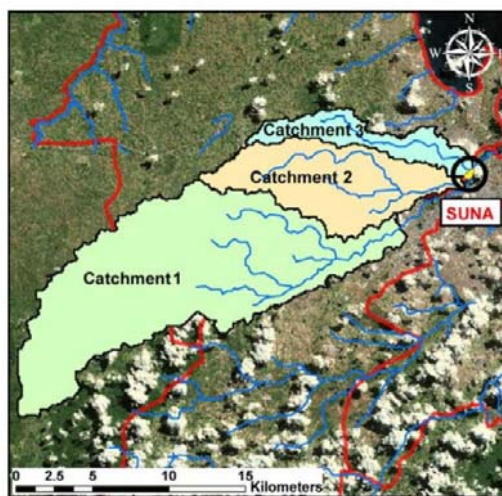


Figure 4. 2: Mizimbazi catchments

The characteristics of the three catchments shown in the pictures are reported synthetically reported in Table 4. 2.

Characteristics	Catchment 1	Catchment 2	Catchment 3
Drainage area (km ²)	166.3	60.5	24.1
Main channel length (km)	32.7	18.2	14.9
Average slope (%)	5.8	4.2	3.9
Average height (m.a.s.l.)	175.5	108.6	97.2
CNII	64.73	77.98	89.91
t _p (h)	13.03	6.90	4.43

Table 4. 2: Characteristics of Mizimbazi river catchments.

To know the value of peak flow of the catchments is been used the Curve Number method both for the historical rainfall data and climate projections. This method is been applied for six different return periods: 2, 10, 30, 50, 100, 300 years. Hydrographs for catchment 1 (with and without climate change effects) are illustrated in Figure 4. 3:

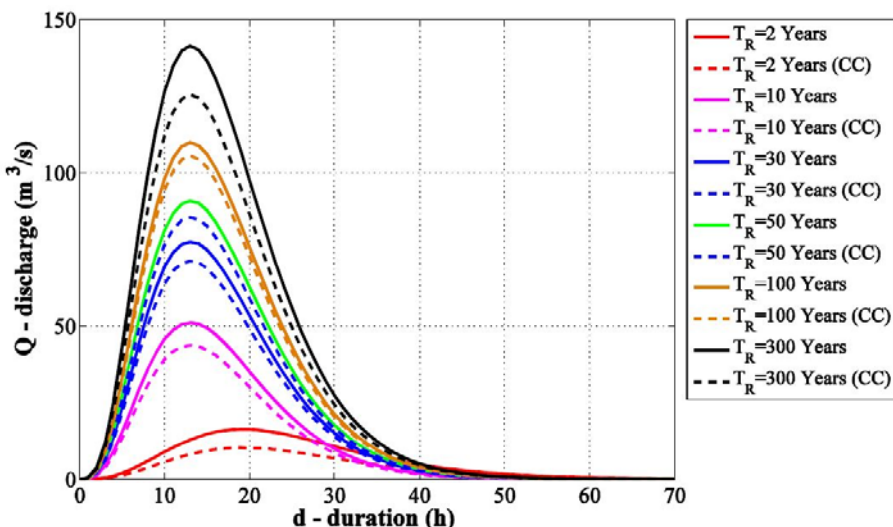


Figure 4. 3: Hydrographs evaluated for catchment 1

Hydrographs are coherent with the IDF curves (Figure 4. 1) because from Figure 4. 3 it is possible to observe that the effects induced by the climate change are lower than the effect produced using the historical rainfall data.

4.1.3 MICRO-SCALE FLOOD HAZARD

To propagate the flooding volume it is lead a bi-dimensional simulation with the software FLO-2D. The simulation is based on hydrographs and the digital elevation model (DEM) and have 45 hours of duration (the total duration of the hydrograph).

Hydrograph used to flooding propagation simulation is referred to historical data without considering the climate change effects. The results of the flood propagation are illustrated in Figure 4. 5 (in terms of maximum flow depth) and in Figure 4. 6 (in terms of maximum flow velocity) with reference to the six return periods considered. The results of flooding propagation simulation referred to climate change effects are not reported in this thesis because they are very similar to those based on historical data.

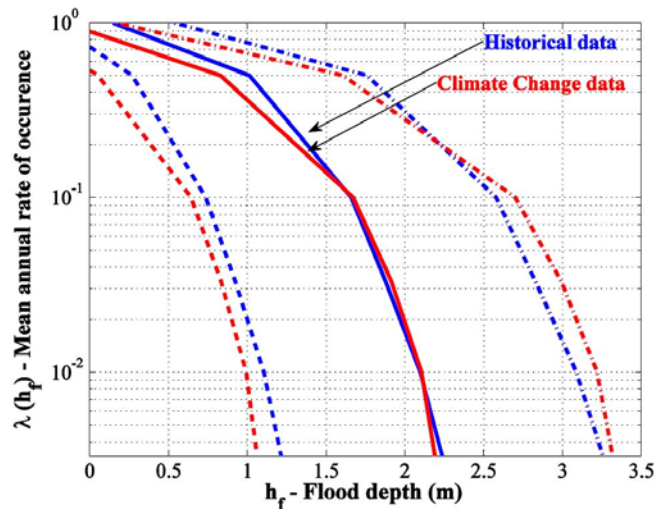


Figure 4. 4: Overlaying representative (mean and mean +/- standard deviation) hazard curves obtained based on, historical data (blue curves) and climate projections (red curves).

Figure 4. 4 represents an overlaying, for a representative building, of the hazard profile in terms of flood depth based both historical data and climate change projections. From the picture it is possible to observe that the hazard values obtained based on historical data are larger with respect to those values obtained considering the climate projections (between 2010-2050). Consequence of this observation is that the hazard curve based on historical data represents a danger grade major than the same evaluated on the hazard curve based on climate change projection so that, a precautionary risk assessment may be leads only on historical data hazard based on.

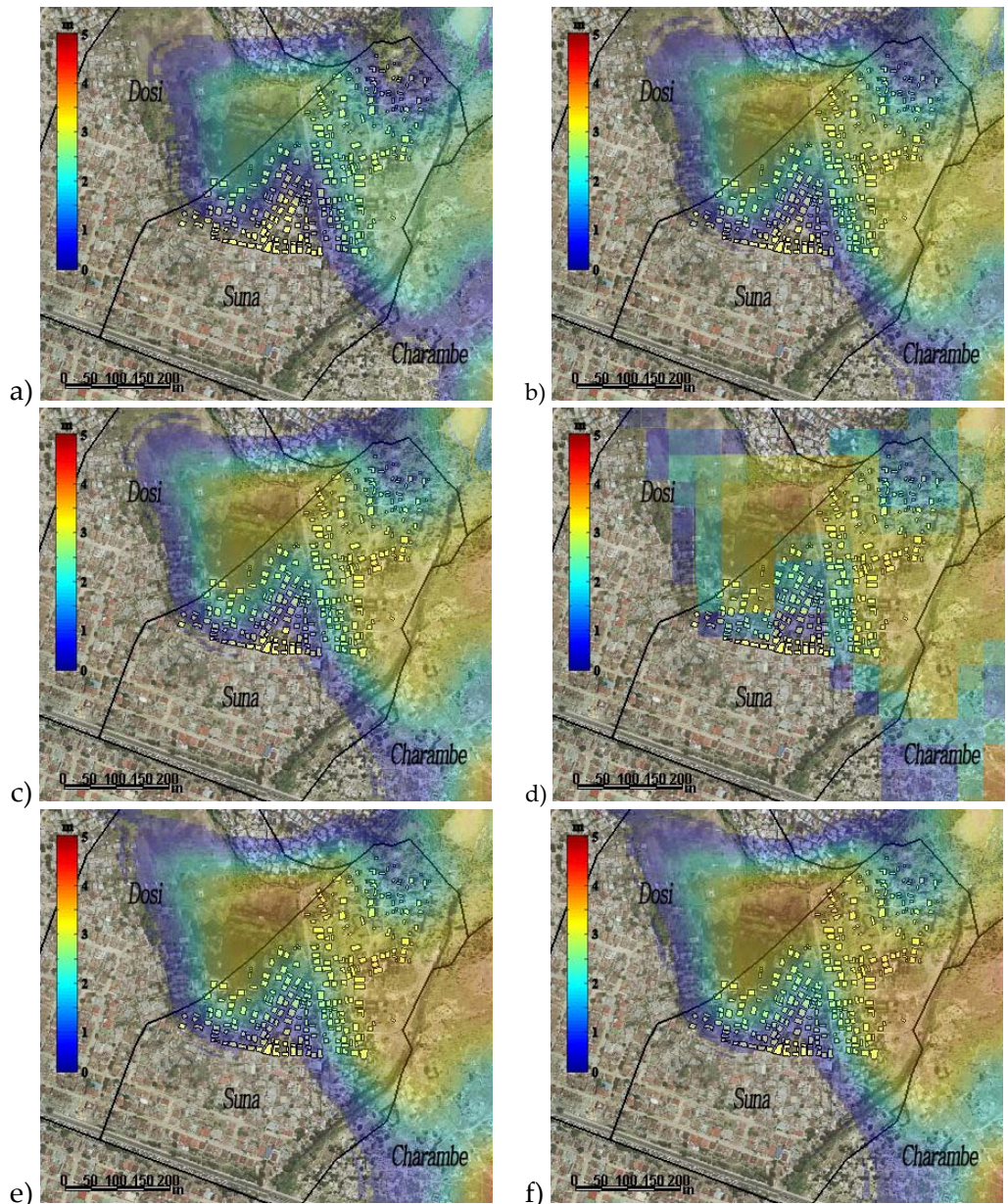


Figure 4. 5 – Inundation profiles for different return periods, based on historical data, in terms of h_{max} : a) $T_R=2$ years, b) $T_R=10$ years, c) $T_R=30$ years, d) $T_R=50$ years, e) $T_R=100$ years, f) $T_R=300$ years.

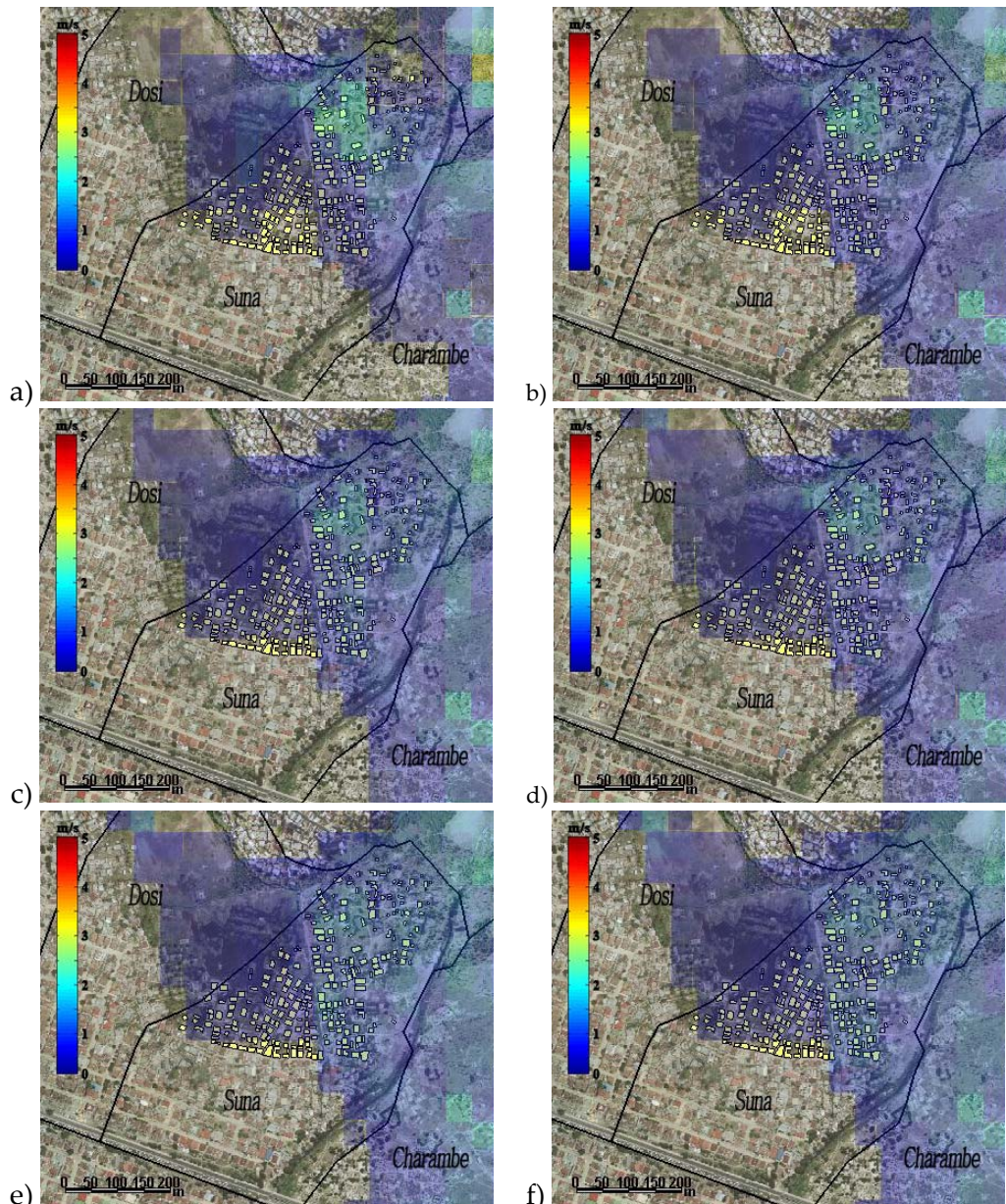


Figure 4. 6 – Inundation profiles for different return periods, based on historical data, in terms of v_{max} : a) $T_R=2$ years, b) $T_R=10$ years, c) $T_R=30$ years, d) $T_R=50$ years, e) $T_R=100$ years, f) $T_R=300$ years.

4.2 Characterization of uncertainties

Suna, located on the western side of the Mismbazi River and on the south side of the Sinza River, with an extension of about 50 ha, is a historical flood-prone area.

The portfolio of buildings object of risk assessment in Suna (Dar Es Salaam) is illustrated in Figure 4. 7. The informal settlements object of risk assessment are identified by an overlaying of the geographic map and the hazard profile in VISK platform. The VISK GIS-based boundary recognition procedure provides the plan dimension of each of the 263 buildings identified in the flood prone area.



Figure 4. 7: Portfolio of the buildings studied in Suna.

The Institute of Human Settlements Studies (IHSS, Ardhi University of Dar Es Salaam) have operated a simple field survey on 100 buildings. The buildings have more-or-less the same characteristics on terms of material used. In particular wall are made with 460x230x125 mm cement blocks; the beams of roofs are generally made of iron or wood. The wall thickness observed throughout the survey operations is around 140 mm (including the width of the plaster if present). Doors types used in the area are of two types: wooden doors and iron doors. Wooden doors are considered not waterproof while iron doors have a very good preventing infiltration capacity. Windows are generally without glass panel and are covered by a nets or plastic sheets so that have not a waterproof capacity.

Case study: Suna

The mechanical model, made up the mechanical properties of materials, is based in existing literature for the cement bricks surveyed. The value of mechanical properties are synthesized in Table 4. 3.

Material Type	f_m (MPa)		τ_m (MPa)		E (MPa)		G (MPa)		γ (MPa)
	Min	Max	Min	Max	Min	Max	Min	Max	
Hollow space 45% - 65%	1.5	2.0	0.095	0.12	1200	1600	300	400	12
Hollow space < 45%	3.0	4.4	0.18	0.24	2400	3520	600	880	14

Table 4. 3: Cement stabilized blocks available in literature [X].

With references to paragraph 2.1.3, to define the logic tree simulation models it is necessary to characterize the uncertainties related at the structural details (discrete binary uncertainties parameters), at the geometry, mechanical and loading properties (continuous uncertainties parameters).

The discrete binary uncertain parameters considered with the related surveyed value are reported in Table 4. 4. The uncertain variables are: presence of raised foundation or presence of a platform (*Pl*), presence of barrier (*Ba*), water-tightness of the doors (*DS*), water-tightness of the windows (*WS*) and presence of a visual degradation of the buildings. VISK vulnerability assessment module uses the organization of the uncertain variables listed in Table 4. 4. This method confers the possibility of define the correlation between various uncertain parameters so that the logic-tree (Figure 2. 6a) may be realized and quantified.

N° OF SURVEYED BUILDINGS	100
n° of buildings with visual degrading	0
n° of buildings with <i>Pl</i>	30
n° of buildings with <i>Ba</i> given <i>Pl</i>	10
n° of buildings with <i>Ba</i> given not <i>Pl</i>	50
n° of buildings with <i>DS</i> given <i>Pl</i> and <i>Ba</i>	5
n° of buildings with <i>DS</i> given <i>Pl</i> and not <i>Ba</i>	15
n° of buildings with <i>DS</i> given not <i>Pl</i> and <i>Ba</i>	30
n° of buildings with <i>DS</i> given not <i>Pl</i> and not <i>Ba</i>	8
n° of buildings with <i>WS</i> given <i>Pl</i> , <i>Ba</i> , and <i>DS</i>	2
n° of buildings with <i>WS</i> given <i>Pl</i> , not <i>Ba</i> , and <i>DS</i>	5
n° of buildings with <i>WS</i> given not <i>Pl</i> , <i>Ba</i> , and <i>DS</i>	10
n° of buildings with <i>WS</i> given not <i>Pl</i> , not <i>Ba</i> , and <i>DS</i>	3

<i>N° OF SURVEYED WALLS</i>	400
<i>n° of walls with D</i>	100
<i>n° of walls with W given D</i>	80
<i>n° of walls with W given not D</i>	200

Table 4. 4: Structural detailing parameters expressed as discrete binary uncertain variables.

The probability π that each logical statement of table Table 4. 4 have a *true value* can be evaluated from complete Beta-function in Equation (2. 6), based on a number n of field survey sheets. There are three possibility to estimate π : a) using the mode of the distribution ($\pi=r/n$); b) using the expected value $\pi=(r+1)/(n+2)$ or c) sampling directly from the probability distribution.

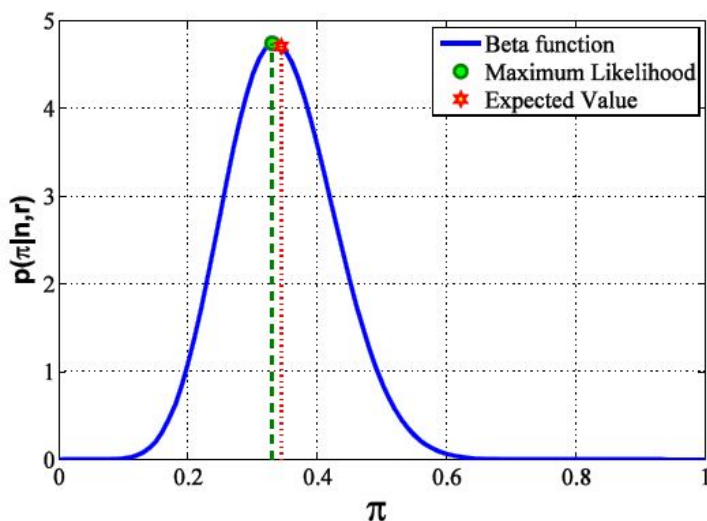


Figure 4. 8: Three alternative possibilities for estimating the probability that the buildings has a platform.

Table 4. 5, Table 4. 6 and Table 4. 7 reports the continuous uncertain parameters divided in three categories: (1) parameters related to the building geometry; (2) parameters related to the mechanical properties; (3) parameters related to the modelling of flood action.

No correlation between parameters has been considered. Wall thickness is assumed to be deterministic and equal to the thickness of the cement bricks.

Normal distribution of probability for the wall length and the foundation raise is obtained from the histogram of the observed data from the survey results.

Uniform distribution of probability is used for all the parameters for which is known only the variation range (i.e., a lower and upper bound).

Only parameter b of flood action models is characterized as an uncertain parameter because the parameter a is completely correlated with b through the relationship expressed from the Equation (2. 5).

Geometrical property	Distribution type	Mean Min	St. Deviation Max
L [m] – wall length	Normal	11.17	3.39
H [m] – wall height	Uniform	2.50	3.50
t [m] – wall thickens	(deterministic)	0.125	0.00
L _w [m] – windows length	Uniform	0.80	1.20
H _w [m] – windows height	Uniform	0.80	1.00
H _{wfb} [m] – windows raise	Uniform	0.80	1.20
L _d [m] – door length	Uniform	0.80	1.20
C _d [m] – corner length	Uniform	0.80	0.90
H _f [m] – foundation raise	Normal	0.45	0.15
H _b [m] – barrier height	Uniform	0.10	1.00

Table 4. 5: Continuous uncertain parameters related to buildings geometry.

Mechanical property	Distribution type	Mean Min	St. Deviation Max
f _m [MPa] – compression strength	Uniform	1.50	2.00
τ_0 [MPa] – shear strength	Uniform	0.095	0.12
f _f [MPa] – flexural strength	Uniform	0.14	0.40
E [MPa] – linear elastic modulus	Uniform	1200	1600
G [MPa] – shear elastic modulus	Uniform	500	667
γ [kN/m ³] – self weight	Uniform	11	13

Table 4. 6: Continuous uncertain parameters related to mechanical properties.

Load property	Distribution type	Median Min	St. Deviation Max
b	Lognormal	1.57	0.54
a	Fully correlated with b [Eq. (2. 5)]		
IT [s] – time of impact	Uniform	0.5	1.5
IM [kg] – mass of impact	Uniform	200	500

Table 4. 7: Continuous uncertain parameters related to loading parameters.

4.3 Vulnerability assessment: analysis and fragility curves

To evaluate the vulnerability of the portfolio of buildings, in add to the uncertain parameters classified at paragraph 4.2, are been chosen for the analysis these other deterministic parameters:

Parameter	Value
Nominal critical water height [m]	1.00
Roof vertical load [kN/m]	0.50
Roof horizontal load [kN/m]	0.00
Rate of openings into wall [n°/m]	0.33
Drag coefficient [-]	2.00
Rate of degradation	0.75

Table 4. 8: Other parameters to analysis.

The wall restrain conditions considerate in these analysis are: hinged sections at the wall sides, fixed section at the bottom of the wall and free section at the upper side of the wall.

In the follows paragraphs are lead e series of comparisons between the fragility curves obtained in different modes. In particular are considered: (a) the differences between three sets of analysis with the same input data and different number of simulation (10, 50 and 100 simulations); (b) the differences between two sets of 10 and 50 analysis characterized by different extraction mode of the uncertain parameters (Maximum Likelihood and Entire Distribution); (c) the difference between the cumulative distributions of probability (normal or lognormal); (d) the difference between the water load (static, dynamic or dynamic plus debris impact) in terms of fragility curves.

4.3.1 EFFECT OF ANALYSIS NUMBER IN VULNERABILITY ASSESSMENT

To evaluate the effects produced by three different number of analysis, in terms of fragility curve, are set in VISK platform the *maximum likelihood* extraction options and the water load as *hydrodynamic plus debris impact*. The fragility curves, follows reported, are obtained as *Lognormal Cumulative Distribution of Probability*. The comparison is made for the Serviceability and Collapse limit states.

Figure 4. 9 reports the robust fragility curves evaluate at Serviceability limit state respectively for 10, 50 and 100 simulations.

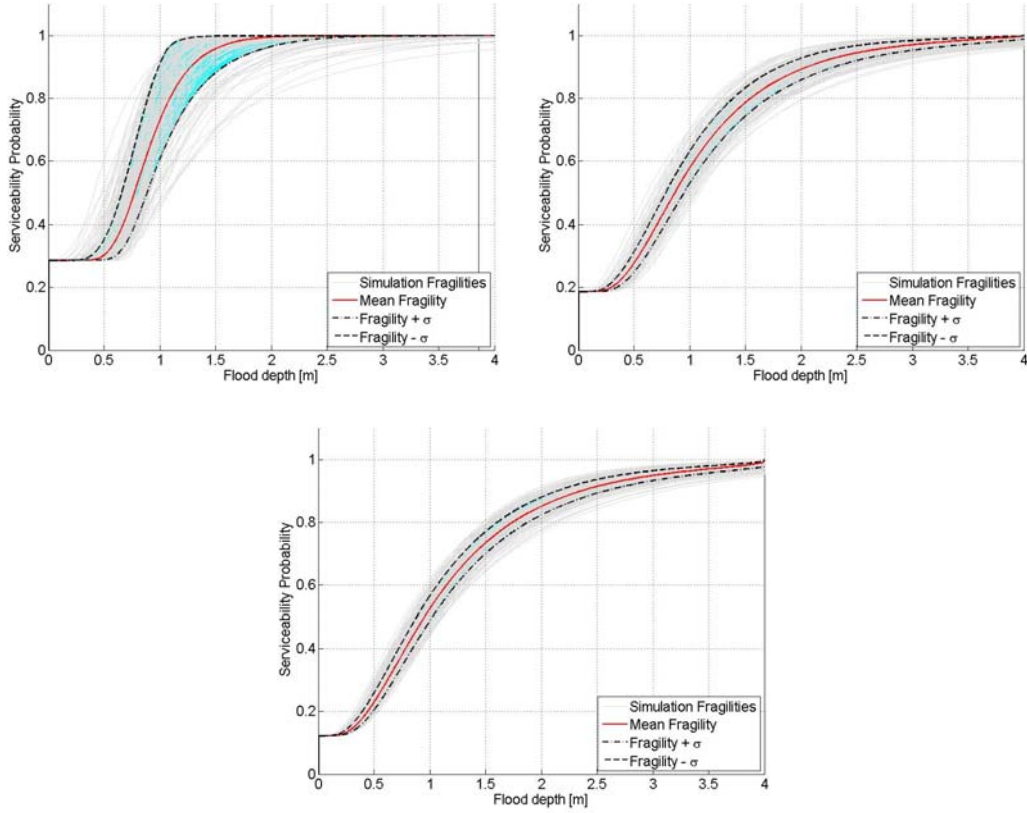


Figure 4. 9 - Robust fragility curves at SE limit state: (I) 10 simulations; (II) 50 simulations; (III) 100 simulations.

A first consideration is about the initial step of the curve. It represents the percentage of simulations for which the critical water height is equal to zero. The pictures denote that this percentage is sensitive to the number of simulations but beyond 50 simulations the difference (in terms of initial steps is not very important). A second consideration is about the curvature change of the plotted functions. At the increases of the simulation number, the curve are more regular symptom of a raise of data on which fragility curve is obtained.

Figure 4. 10, instead, reports the robust fragility curves at Collapse limit state.

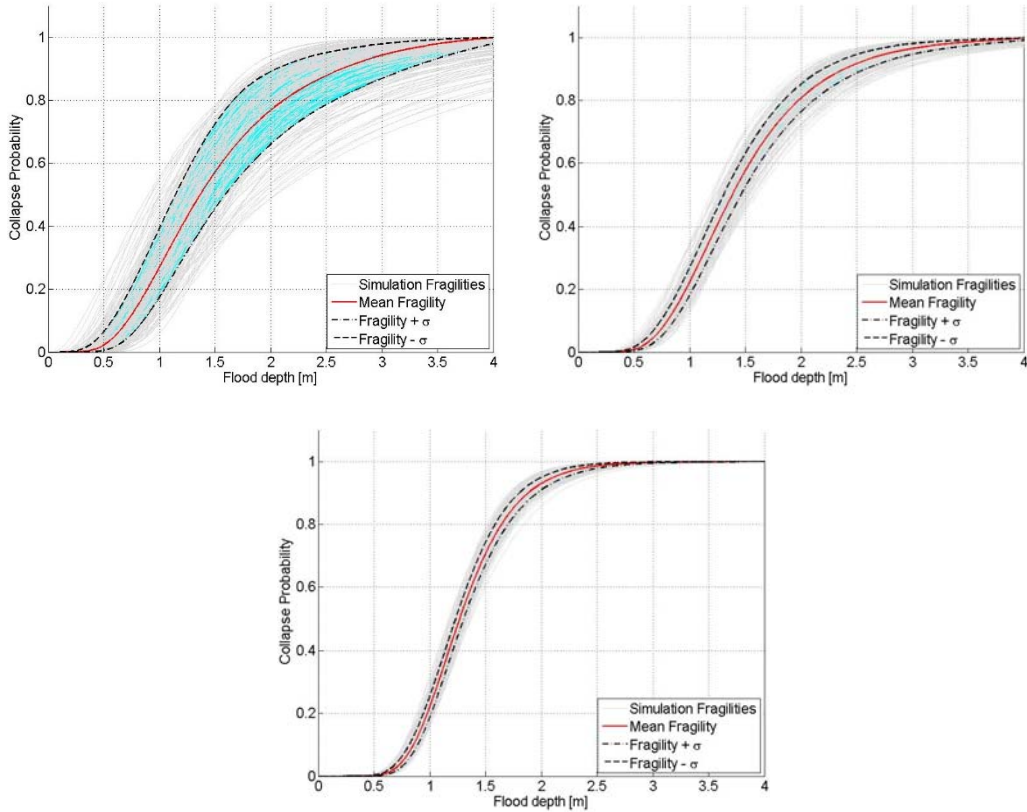


Figure 4. 10 - Robust fragility curves at CO limit state: (I) 10 simulations; (II) 50 simulations; (III) 100 simulations.

Both in Serviceability and Collapse limit states, the plotting of robust fragilities shows that the confidence interval (fragility +/- standard deviation) is very large in case of 10 simulations and it decrease when the number of simulations increase. So, the substantially differences between the vulnerability assessment obtained with different number of simulation is the precision of the vulnerability value and a reduction of the confidence interval. These lasts improve with increasing of the analysis number but the difference between the vulnerability evaluated with 50 analysis and 100 analysis is not substantially different. So that 50 analysis is a good compromise between the vulnerability assessment accuracy and the analysis time.

4.3.2 EFFECT OF EXTRACTION CRITERIA IN VULNERABILITY ASSESSMENT

The effect of extraction criteria is evaluated on two sets of 10 and 50 simulations with the parameters defined at paragraphs 4.2 and 4.3, executed

both with maximum likelihood and entire distribution as criteria of extraction of the uncertain parameters. The results are compared in terms of fragility curve plotted for the three limit states considered.

Figure 4. 11 reports the overlaying of the median fragility curves evaluate with an analysis of 10 simulations. In red colour is plotted the curve obtained with the maximum likelihood criteria of extraction and in blue colour the curve obtained with the entire distribution considered for the uncertain parameters.

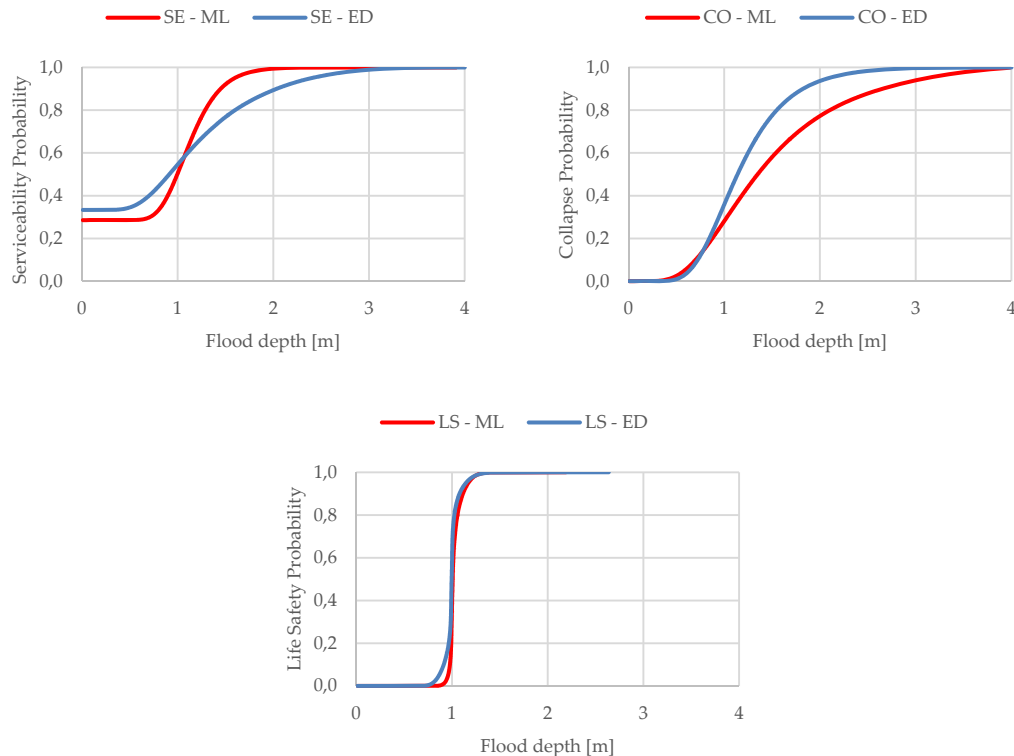


Figure 4. 11 – Overlay of the median fragility for the three limit state considered for two typology of extraction with 10 analysis simulations.

Fragility curves in case of Serviceability and Collapse limit state presents a substantial difference depending by the extraction criteria; in case of Life Safety this difference is not very important.

Figure 4. 12 represents the overlaying of the median fragility curves evaluate with an analysis of 50 simulations. These pictures shows that the difference in terms of vulnerability assessment is absolutely irrelevant for an evaluation based on 50 simulations.

Both in the case of 10 and 50 simulations number the fragility curves for Life Safety limit state are not very different because, the vulnerability assessment in this limit state is strongly dictated by the nominal value of critical water height contrary to what happens to the other two limit states.

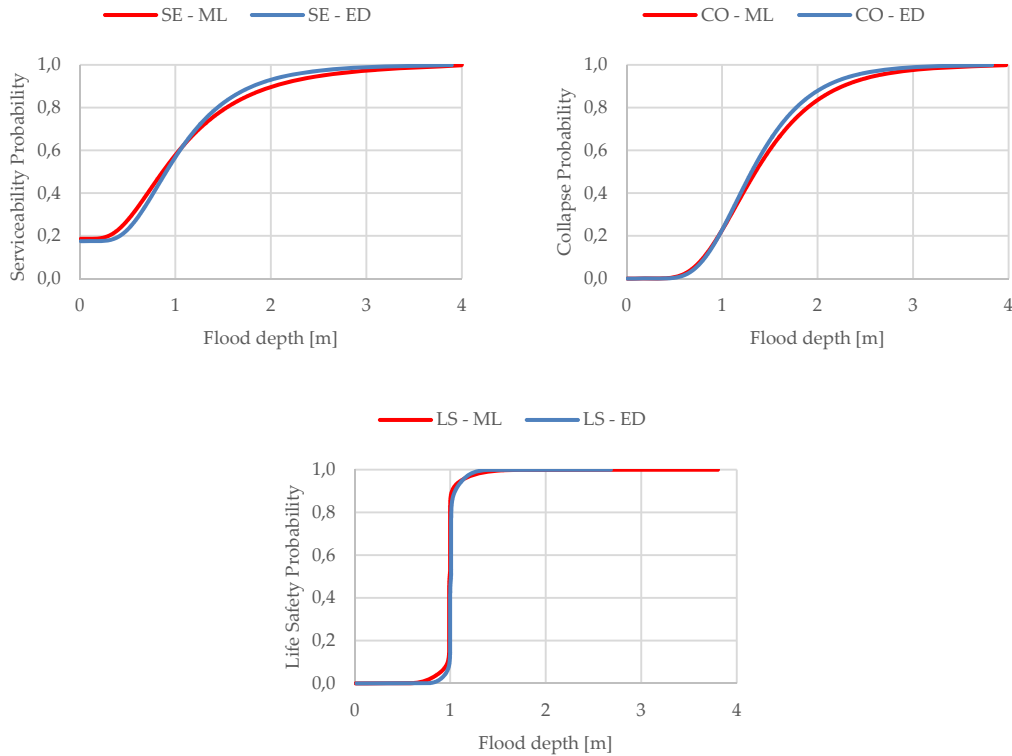


Figure 4. 12 – Overlay of the median fragility for the three limit state considered for two typology of extraction with 50 analysis simulations.

After these considerations, in add to how expressed at paragraph 4.3.1, the number of simulation that is a good compromise between: minimum analysis time, minimum confidence interval and better influence of extraction criteria of parameters is 50.

4.3.3 EFFECT OF DISTRIBUTIONS PROBABILITY IN VULNERABILITY ASSESSMENT

To evaluate the effects of distribution probability typology (normal or lognormal) are executed 50 simulations characterized by the parameters defined at paragraphs 4.2 and 4.3 in which, the uncertain parameters, are extracted as maximum likelihood value.

Figure 4. 1 represents the robust fragility curves, evaluated at the Collapse limit state, with 50 simulations considering a normal cumulative distribution of probability (in the left pictures) and a lognormal cumulative distribution of probability (in the right picture).

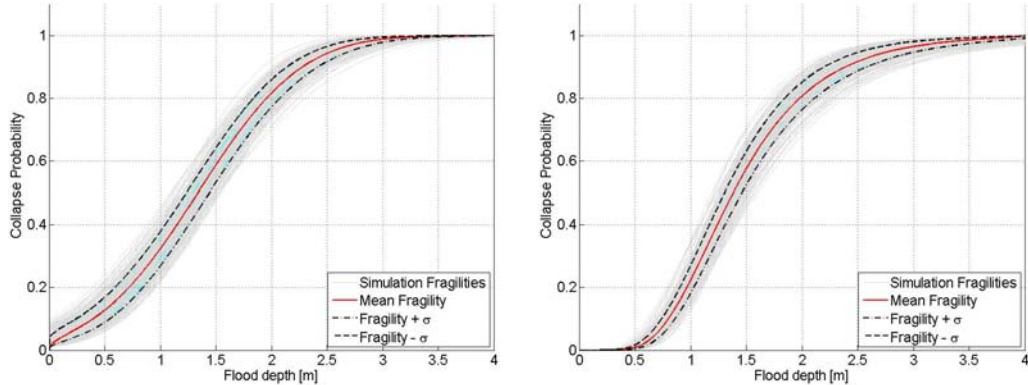


Figure 4. 13 - Robust fragility curves at CO limit state obtained based on 50 simulations: (left) Normal Cumulative Distribution of probability; (right) LogNormal Cumulative Distribution of probability.

The difference between the two curves may best be appreciated observing Figure 4. 14 where are plotted on the same axis the lognormal and normal fragility curves obtained with VISK calculation and the Empirical Cumulative Distribution Function evaluated with the vector of critical water height at the collapse limit state.

Figure 4. 14 shows that the fragility curve evaluated through VISK platform considering a lognormal distribution of probability is the one that best approximate the Empirical Cumulative Distribution Function. This approximation improves when the analysis number increase but already for 50 simulation the approximation is satisfactory.

In add to the considerations made above, Figure 4. 15, depicts that the empirical cumulative distribution is very well contained into the confidence interval delimited by the median fragility +/- one standard deviations.

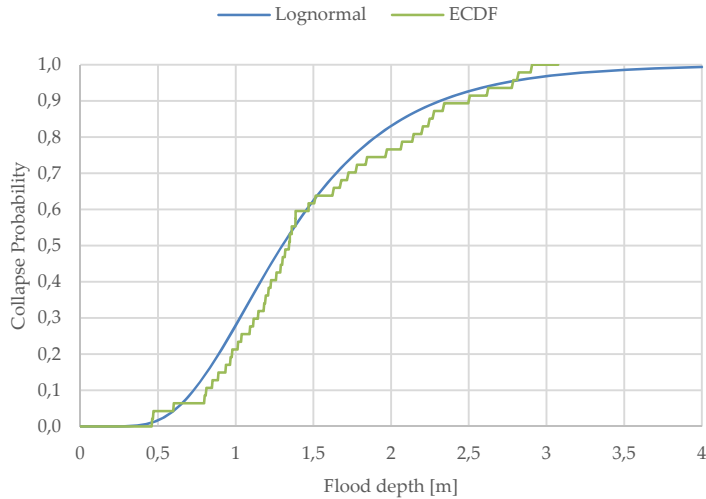


Figure 4. 14: Overlaying of Normal, Lognormal and ECDF fragility curves.

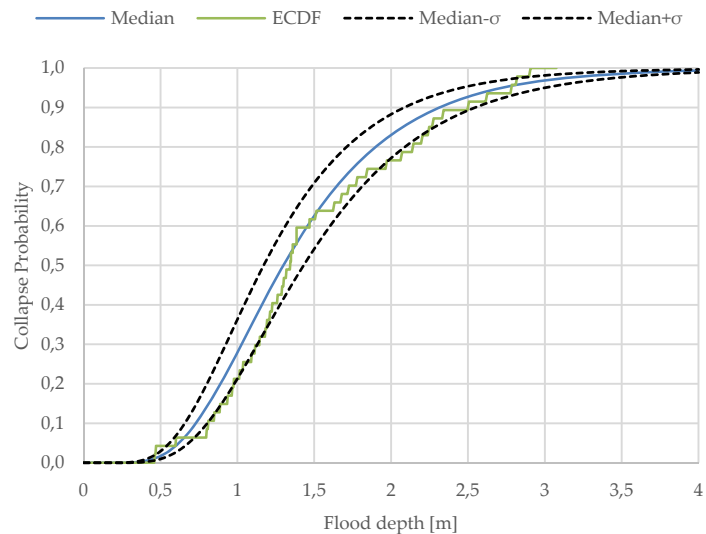


Figure 4. 15: Overlaying of ECDF and confidence interval.

4.3.4 EFFECT OF WATER LOAD IN VULNERABILITY ASSESSMENT

The objective of this paragraph is to demonstrate the effect of the water load type (hydrostatic, hydrodynamic or hydrodynamic plus debris impact) on the four model of wall considered (ref. Figure 2. 10) with two restrain condition: (a) hinged sections at the wall sides, fixed section at the bottom of the wall and

free section at the upper side of the wall; (b) fixed sections at the wall sides and at the bottom of the wall and free section at the upper side of the wall.

The methodology with which VISK defines the structural model of the wall at j -th simulation is based on the logic tree approach explained at the paragraph 2.1.3. This way of proceeding lead to a vulnerability assessment based on a fragility curve evaluated on the combination of different structural models of wall defined obtained from the probabilistic consideration of the binary uncertain parameters. For this reason, to evaluate a fragility curve based on the analysis of the continuous uncertain parameters on a fixed wall model, it is necessary to change the binary uncertain parameters in order to have a logic tree that lead to the opportune wall model.

The comparison between the various wall models, with different water-load and support conditions, is made at the Collapse limit state so that, to evaluate in the better manner the effect of the water load it is necessary to consider always the absence of the platform and barrier and a waterproof closure system (characterized by sealed doors and windows).

Table 4. 9 reports the values of binary uncertain parameters (related to the entire building) set in VISK in order to have a buildings model that prevent the water entry inside the building. In this manner it is possible to evaluate correctly the water load effect during the vulnerability assessment.

<i>N° OF SURVEYED BUILDINGS</i>	100
n° of buildings with visual degrading	0
n° of buildings with <i>Pl</i>	0
n° of buildings with <i>Ba</i> given <i>Pl</i>	0
n° of buildings with <i>Ba</i> given not <i>Pl</i>	0
n° of buildings with <i>DS</i> given <i>Pl</i> and <i>Ba</i>	0
n° of buildings with <i>DS</i> given <i>Pl</i> and not <i>Ba</i>	0
n° of buildings with <i>DS</i> given not <i>Pl</i> and <i>Ba</i>	0
n° of buildings with <i>DS</i> given not <i>Pl</i> and not <i>Ba</i>	100
n° of buildings with <i>WS</i> given <i>Pl</i> , <i>Ba</i> , and <i>DS</i>	0
n° of buildings with <i>WS</i> given <i>Pl</i> , not <i>Ba</i> , and <i>DS</i>	0
n° of buildings with <i>WS</i> given not <i>Pl</i> , <i>Ba</i> , and <i>DS</i>	0
n° of buildings with <i>WS</i> given not <i>Pl</i> , not <i>Ba</i> , and <i>DS</i>	100

Table 4. 9: Structural detailing parameters to have a waterproof building models.

After the definition of the building waterproof characteristics, it is necessary to define in VISK the binary uncertain parameters that leads to the

particular wall model of interest in the logic tree for the assessment of fragility curve.

Table 4. 10, Table 4. 11, Table 4. 12 and Table 4. 13 reports the wall binary parameters to have respectively a *solid wall model*, a *wall with door model*, a *wall with windows model* and a *wall with door and windows model*.

For each of these set of parameters (therefore wall model) are lead an analysis campaign to evaluate the effect of the water load and support condition. Each analysis is based on 50 simulations.

<i>N° OF SURVEYED WALLS</i>	400
n° of walls with <i>D</i>	0
n° of walls with <i>W</i> given <i>D</i>	0
n° of walls with <i>W</i> given not <i>D</i>	0

Table 4. 10: Wall detailing to fix "solid wall" in VISK structural model.

<i>N° OF SURVEYED WALLS</i>	400
n° of walls with <i>D</i>	400
n° of walls with <i>W</i> given <i>D</i>	0
n° of walls with <i>W</i> given not <i>D</i>	0

Table 4. 11: Wall detailing to fix "wall with door" in VISK structural model.

<i>N° OF SURVEYED WALLS</i>	400
n° of walls with <i>D</i>	0
n° of walls with <i>W</i> given <i>D</i>	0
n° of walls with <i>W</i> given not <i>D</i>	400

Table 4. 12: Wall detailing to fix "wall with windows" in VISK structural model.

<i>N° OF SURVEYED WALLS</i>	400
n° of walls with <i>D</i>	400
n° of walls with <i>W</i> given <i>D</i>	400
n° of walls with <i>W</i> given not <i>D</i>	0

Table 4. 13: Wall detailing to fix "wall with door and windows" in VISK structural model.

Follows are reported the fragility curves evaluated as above explained. Graphics are coupled in function of the wall model (solid wall, wall with windows, wall with door and wall with door and windows) highlighting the difference between the support condition. In the wall picture, the continuous red lines represent the fixed sections while the dashed red lines represent the hinged sections.

Each graphics depicts the three fragility curves evaluated with the three water load possibility: hydrostatic, hydrodynamic and hydrodynamic plus debris impact.

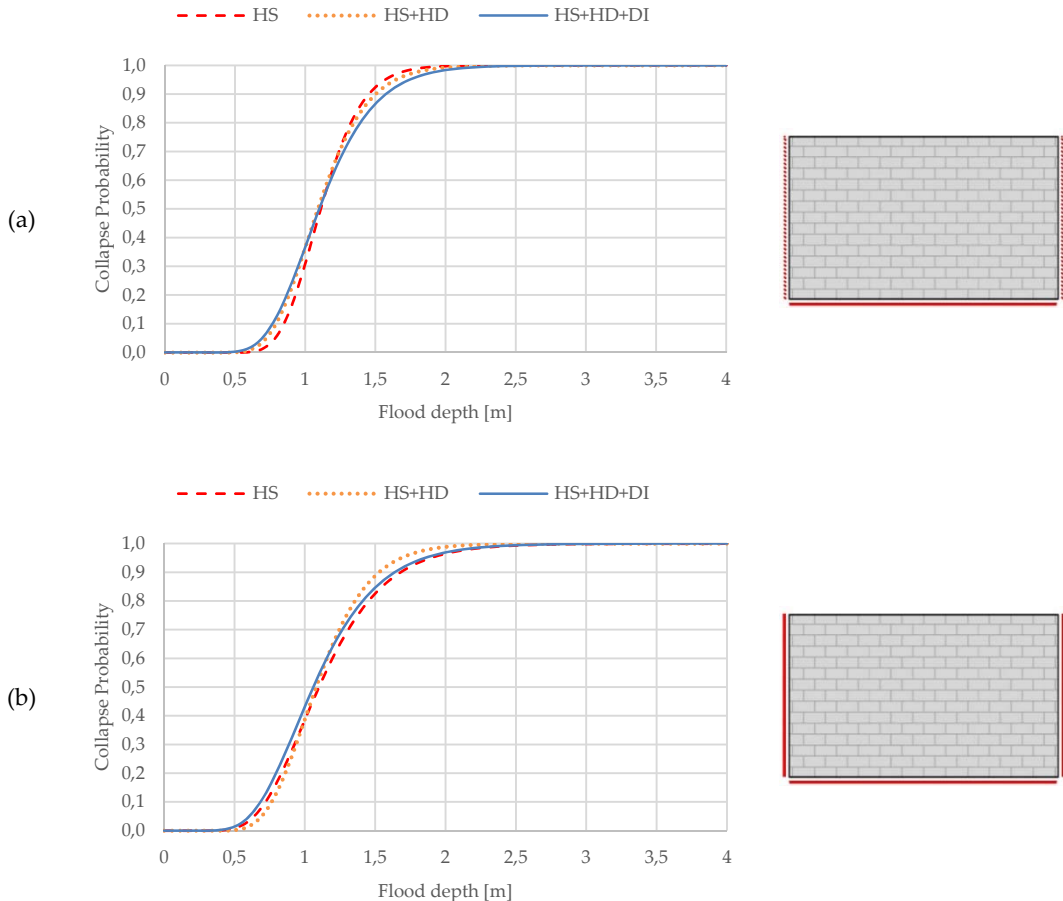


Figure 4. 16 - Fragility curves for three load combination: (a) hinged-fixed solid wall; (b) fixed solid wall.

For the solid wall model the support condition and the water load don't produce substantially effects in terms of fragility curves evaluation.

Figure 4. 16 depicts that, for all the water load conditions, in case of wall with hinged lateral sections, at the increasing of the flow depth, the collapse probability increase with greater rapidly respect at the wall with fixed lateral section.

The difference between the two models is not very relevant because the section where occurs the crisis is always the bottom side of the wall.

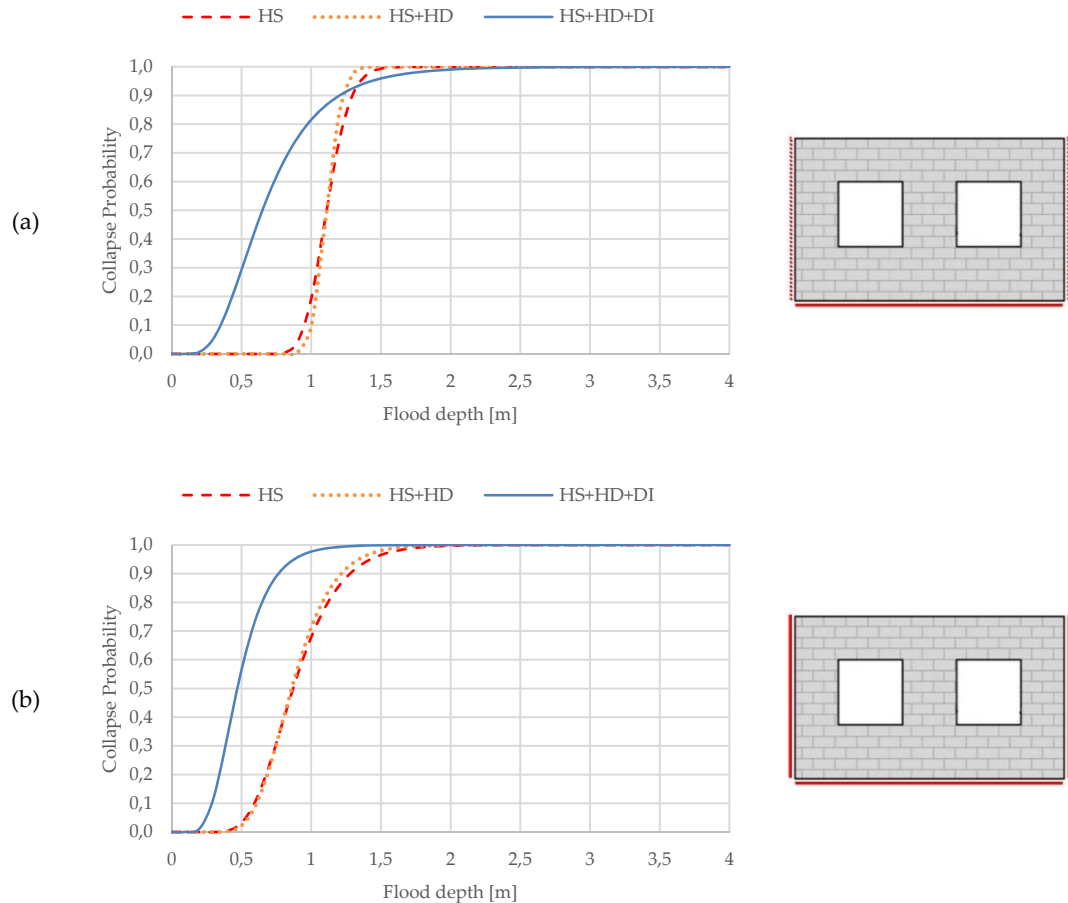


Figure 4.17 - Fragility curves for three load combination: (a) hinged-fixed wall with windows; (b) fixed wall with windows.

Figure 4.17 reports the vulnerability assessment of the wall model characterized by the presence of only windows. The number and the position of windows is randomized by VISK.

The changing of support condition in this model produces some variation of the sections in which the crisis occurs. The more onerous conditions for the wall is produced by the effects of hydrostatic plus hydrodynamic plus debris impact load.

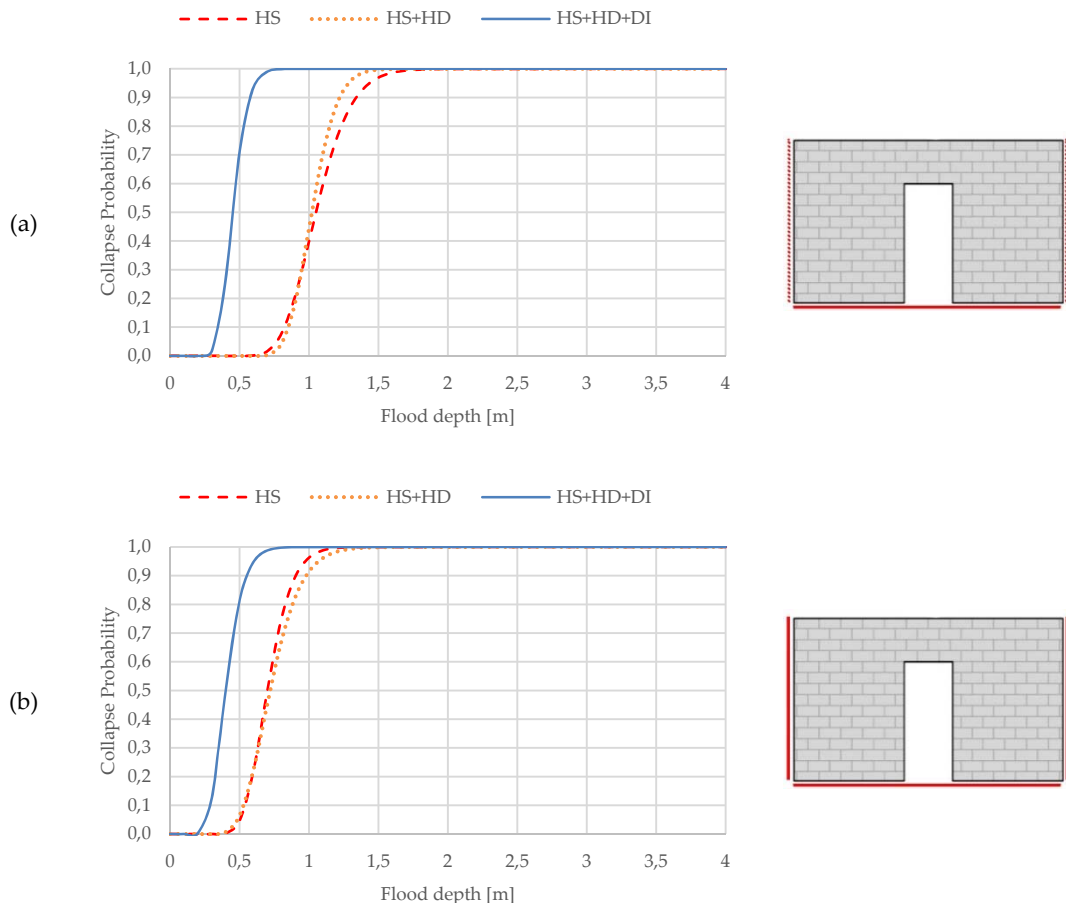


Figure 4. 18 - Fragility curves for three load combination: (a) hinged-fixed wall with door; (b) fixed wall with door.

The fragility curves for the wall model characterized by the presence of only door are reported in Figure 4. 18.

The more onerous conditions for the wall is produced by the effects of hydrostatic plus hydrodynamic plus debris impact load and the fragility curve evaluated in this condition don't change particularly when change the support condition. When load condition is characterized only by hydrostatic or hydrodynamic water load fragility curves have variations depending of the support condition. In particular when the lateral sections of the wall are fixed the collapse probability are larger than the same when the lateral side of the wall are hinged.

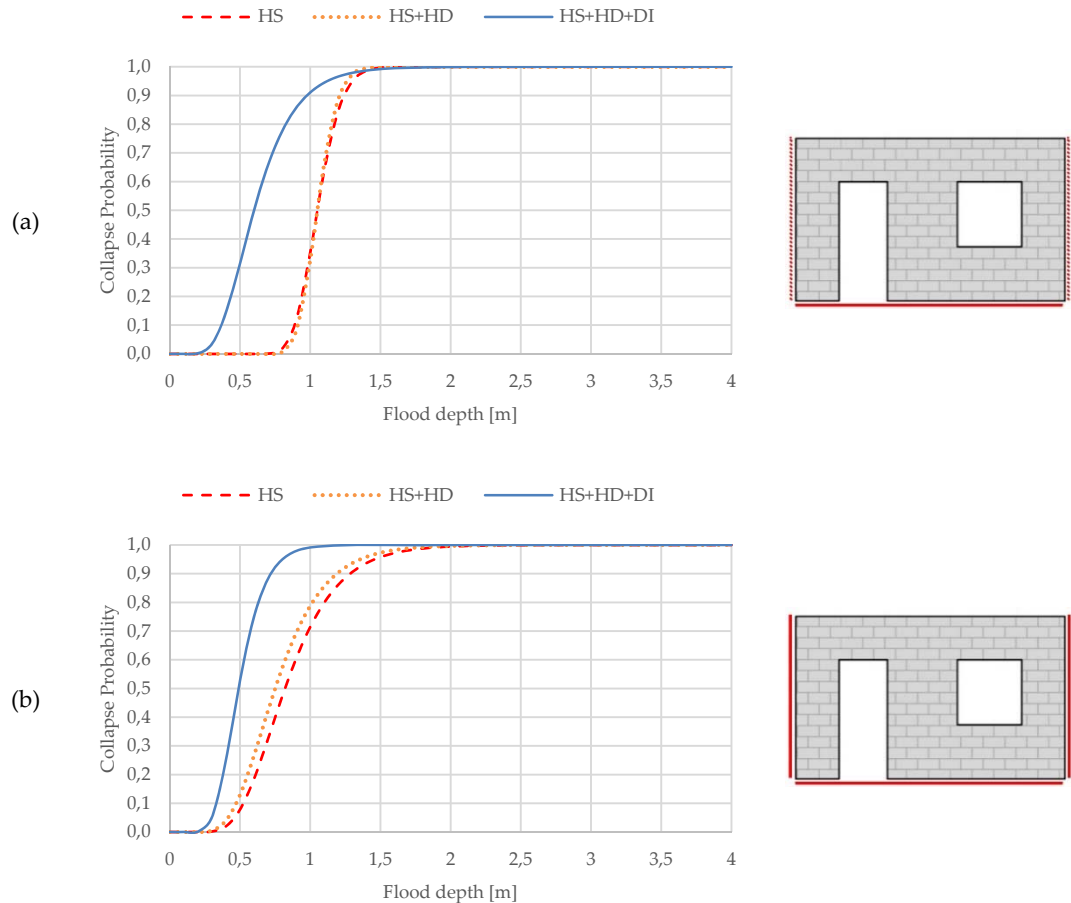


Figure 4. 19 - Fragility curves for three load combination: (a) hinged-fixed wall with door and windows; (b) fixed wall with door and windows.

Also in the case of wall with door and windows (reported in Figure 4. 19), the more onerous conditions for the wall is produced by the effects of hydrostatic plus hydrodynamic plus debris impact load. Collapse probability in case of wall fixed at sides is greater than evaluate for the wall hinged at sides.

An observation of all the fragility curves shows that for the case study area, flooding velocity is not so high as to influence the structural response therefore, the fragility curves for the hydrostatic only and hydrostatic plus hydrodynamic load are quite similar.

It can be observed that debris impact leads to significantly higher fragility values, in the presence of openings. The presence of doors and windows seem

to have undesirable effects on structural performance due to both local stress concentration close to openings and also eventual reduction of resisting section.

4.4 Risk assessment

Risk assessment for the case study area is lead through the using of VISK platform that includes the methodology explained at 2.2.7. After the evaluation of the vulnerability of the portfolio of buildings (in terms of fragility curve) and the consideration of the hazard profile, VISK evaluate building-to-building the flooding risk with the equation (2. 26).

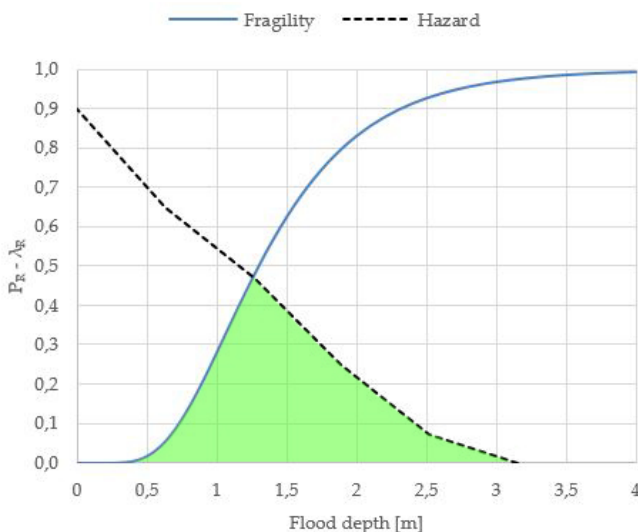


Figure 4. 20: Graphical definition of the risk.

Figure 4. 20 represent the graphical definition of the risk. VISK, in fact, execute building to building the integration operation of the area under the intersection between the fragility curve and hazard curve. VISK generate e colour map based on the value of the risk building-to-building and generate a risk map in which the colour is representative of the risk value of the buildings.

In this paragraph it want to focalize the attention on the risk of flooding at Life Safety limit state. The vulnerability assessment is lead with the parameters established at paragraphs 4.2 and 4.3 through the execution of 50 simulation with the maximum likelihood extraction mode (of the uncertain parameters) and a lognormal distribution of probability is considered to the robust fragility procedure. The fragility curve products is reported in Figure 4. 21.

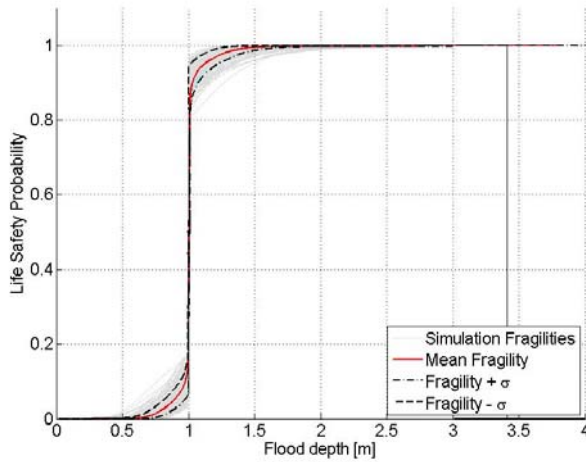


Figure 4. 21: Robust fragility curve at Life Safety limit state.

With reference to the mean fragility (red line of Figure 4. 21) are reported in Figure 4. 22 the risk maps in terms of probability⁵ of exceedance of Life Safety limit state in 1, 2, 5 and 25 years.

The maps evaluated with mean-fragility +/- standard deviation are (just from the graphical point of view) very similar to those evaluated with mean fragility only because the difference between the fragility curves into the confidence interval is exiguous.

In add to the graphical information visible through the risk maps, VISK allows the calculation of the flooding risk in terms of *expected casualties* and *financial losses*. In particular for the case study is considered a number of people to square meter of 0.03 and a cost of reparation/replacement of building affected from flooding problem of 3 € at square meter. The total number of people that live in Suna is (considering 0.03 people/m²) equal to 663.

Table 4. 14 reports, for the four number of years considered, the number of people that risk their life and the value of the financial losses as repair/replacement cost.

⁵ The annual probability of exceeding a limit state $P(LS)$ is evaluated with the Equation (2. 27) assuming a homogeneous Poisson process model.

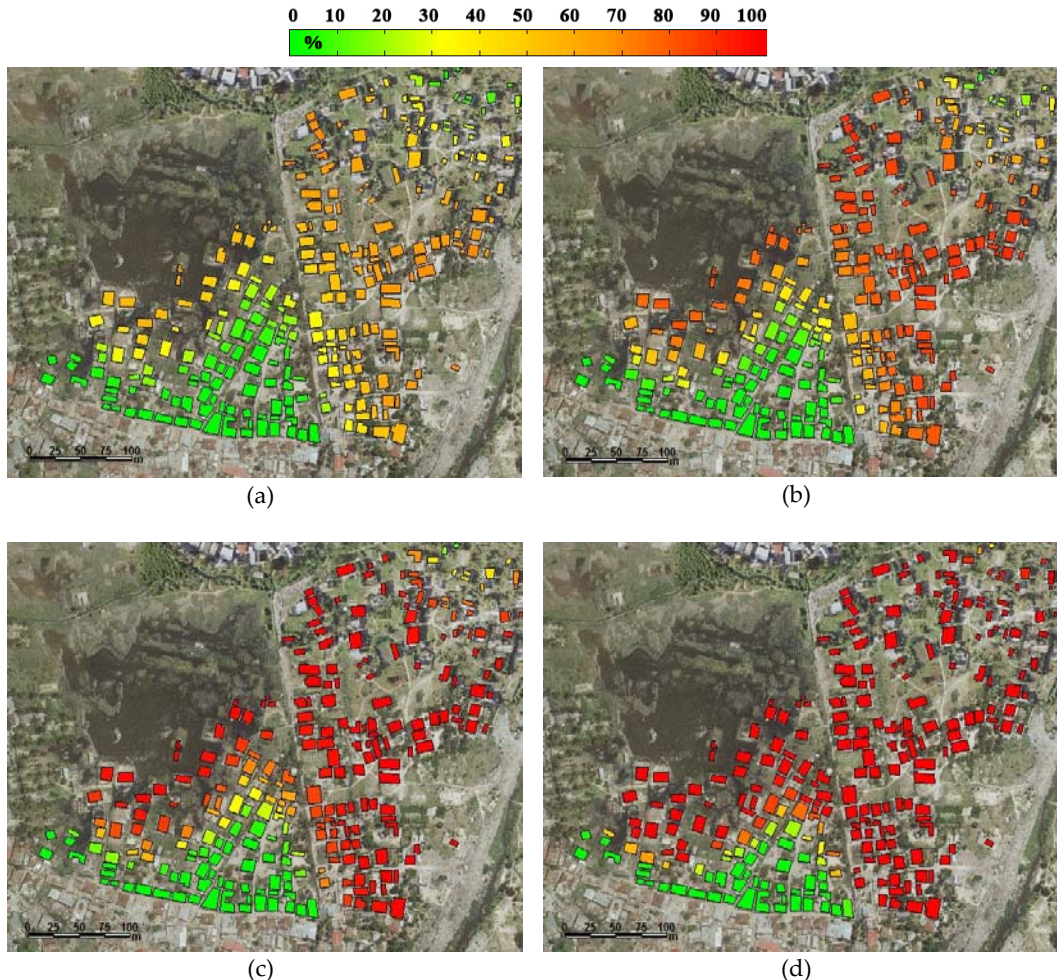


Figure 4. 22 - Risk maps in terms of probability of exceeding the LS limit state: (a) in 1 year; (b) in 2 years; (c) in 5 years; (d) in 25 years.

Year(s)	People at life risk [N°]	Repair/replacement losses [€]	Perc. of the total [%]
1	227	22620	34
2	334	33310	50
5	439	43888	60
25	510	50910	77

Table 4. 14: People at life risk and financial losses.

Chapter 5

FINAL REMARKS

This thesis present a GIS-based software platform to flooding vulnerability and risk assessment of a portfolio of buildings in a micro-scale approach. The software developed during this thesis is called VISK and enclose e Bayesian simulated-based methodology that through the flooding hazard and the vulnerability evaluation arrive to the flooding risk assessment.

Chapter 1 introduces the works treated in the thesis. Are presented the objectives established before the development of the software platform that are: interactively and user friendly interface, visual input/output interaction, exportability of results and customizability. Are also reported in this chapter the preliminary knowledge necessary to realize a software to flooding risk assessment and a synthetic description of the case study area.

Chapter 2 describes the methodology with which it is possible to execute a flooding risk assessment for a portfolio of building in a micro-scale contest starting from the definition of the area of interest of the problem through the orthophoto. This last allows to identify the buildings subjects to flooding problem and their position is reliable because the orthophoto contains GIS information of the areas. Important, to a precise identification of the buildings, is a sufficient resolution of the pictures.

In the flood-prone areas, through the rainfall data (IDF curves), the topography, geological and land use information is possible to construct the hydrographs that represent (to a given return period) the total water discharged in a natural basin due to rain events. The hydrograph and a digital elevation model (DEM) insert into FLO-2D software give the flood hazard profile that are the maximum value of water height and velocity for all the considered return

periods. These values are expressed for a lattice of points representative of the area of interest. The hazard profile are translated in actions on the buildings in terms of hydrostatic and hydrodynamic loads. Also a debris impact may be considered as load on the buildings.

To execute a flood vulnerability assessment on the buildings it is necessary to model them and evaluate their resistance capacity. The Bayesian simulated method used for the assessment consider a series of uncertain parameters: discrete binary variables and continuous variables. The extraction on the first allows to decide the structural model to evaluate (solid wall, wall with door, wall with windows or wall with door and windows); the extraction on the second category of parameters define the dimensions and the mechanical property of the model chosen. The model so defined is schematized in OpenSes code as a bi-dimensional elements and a finite-elements-method analysis is due to evaluate the bearing capacity of the structure in terms of critical water height. The vulnerability of the portfolio of building is expressed by the robust fragility curves. These functions are evaluated as the statistics (16th, 50th and 84th) of a series of fragility curves simulated taking in to account the uncertainties above mentioned. The definition of the fragility functions depends of the limit state, in fact, it is possible to evaluate the vulnerability at Serviceability (SE), Collapse (CO) or Life Safety (LS) limit state. SE is reached when the water enter inside the buildings; CO is determined from the failure of the resistant mechanism of the structure that occur when in one of the critical sections the maximum stress capacity (produced by flexure or shear mechanisms) is exceeded; LS is reached when water height exceed the minimum value between the water height that produce the collapse of the structure and a nominal water established as soil of life dangers.

Flooding micro-scale risk assessment of a portfolio of building is performed through the building-to-building integration of the flooding hazard curve and the robust fragility curves. Flooding risk is expressed in different modes: the mean annual frequency of exceeding a given limit state, the probability of exceeding a limit state in a given number of years, the expected number of casualties and the expected replacement/reconstruction costs.

Chapter 3 has the objective to introduce the VISK software platform. The graphic interface is descripted in detail, the panels that include the input and

output function are singularly explained in all their parts. On the left side of VISK interface there are the main input functionalities as the loading panel of orthophotos, hazard profiles and buildings shape. In the middle there are the maps windows and the panel with which buildings may be identified through the recognition of their boundaries. On the right side, instead, are present the panel with all the definitions for the analysis procedures, the fragility curve evaluation functions and the maps creation panel.

The workspace is initialized with the loading of the maps of the interest area and the hazard profiles for all the return periods considered in terms of water height and velocity. The following operation to execute is the identification of the buildings on the map with through the acquiring panel. The numerical definition of all the uncertain parameters allows to do the analysis. The fragility curve may be evaluate in the robust manner with the analysis results for a given limit state or may be created by the user in a fully-customizable mode. The risk assessment may be expressed in different modes: as the mean annual rate or probability in a given number of years. Risk result may express the limit state exceeding, the expected causalities or the replace/reconstruction costs.

VISK results are exportable as images of the risk maps or as shape file importable in whatever GIS-based software platform.

Chapter 4 reports an example of the application of the entire methodology of risk assessment, executed with VISK platform, for the portfolio of buildings in Suna (Dar Es Salaam in Tanzania). This risk assessment is leaded in range of the European FP7 project of CLUVA (Climate Change and Urban Vulnerability in Africa).

The definition of the rainfall curves for the case study area is based both on the historical data (1958 – 2012) and on climate change projection for 2050. These data are used to evaluate the hydrographs for six return periods: 2, 10, 30, 50, 100 and 300 years. Through the software FLOW-2D the hydrographs are studied in a bi-dimensional diffusion model where the equations of motion and continuity are integrated. The value of water height and velocity are evaluated for the six periods of return both for the historical data and the climate change projections. Through the overlaying of the hazards (historical and climate

change data) is been possible to highlight that the climate change effects in terms of flooding hazard may be neglected.

The uncertain parameters of the portfolio of 263 buildings (related to the waterproof characteristics of the closure systems, the geometry and the materials) are evaluated based on a detailed field survey of 100 buildings. The distribution of the continuous uncertain parameters is considered uniform except for the length of the walls, the foundation raise (considered normal) and the wall thickness (consider as a deterministic value).

The vulnerability assessment is executed in various ways. Were performed various analysis scenario to determinate the influence in terms of fragility curves of: the numbers of simulation (10, 50 or 100 simulations), the extraction criteria (maximum likelihood or entire distribution), the distribution of probability in vulnerability assessment (normal or lognormal) and the water load (hydrostatic, hydrostatic plus hydrodynamic, hydrostatic plus hydrodynamic plus debris impact). The analysis has demonstrate that the better compromise between the analysis time and the results reliability is reached on 50 analysis with the maximum likelihood extraction criteria characterized by a hydrostatic plus hydrodynamic plus debris impact load and a lognormal probability distribution to evaluate the fragility function.

Flooding risk assessment for the case study area is executed in terms of probability of exceeding the Life Safety limit state in 1, 2, 5 and 25 years. The results are alarming because already in 1 about the 34% of people risk their life. This percentage become of about the 77% in 25 years.

Chapter 5 is the current where a summary of the entire thesis and the possible future developments are reported.

The development of VISK platform is been focalized only for the micro-scale flooding risk assessment for one class of a portfolio of buildings. The methodology applied in this thesis may be revisited to enlarge the potentiality of VISK in four main ways.

The **first** possible future develop regards the integration of an hydraulic calculation routine inside the platform so that it is no longer necessary to use another software.

The **second** possible future develop regards the possibility of extend the risk assessment to more classes of buildings simultaneously. It is frequent that in a flood-prone area there are different typology of buildings subjected to flooding problem. VISK will provide the possibility to assign a different class of uncertain to buildings with different characteristics. The analysis procedure will be revisited to this new purpose to evaluate correctly the vulnerability of the portfolio of buildings.

The **third** possible future develop regard the scale in which the risk is evaluated in VISK platform. If the flood hazard is based on a geo-spatial dataset of potentially flood prone urban areas, called the Topographic Wetness Index (TWI) map, the flood-prone areas are identified by a TWI larger than a certain threshold. A GIS-based Bayesian parameter-estimation method may be develop in order to estimate the TWI threshold based on the inundation profiles calculated for one or more micro-scale spatial windows. By the overlaying of the TWI with the UMT (Urban Morphology Types) it is possible to evaluate the urban area at flooding risk. This is a meso-scale risk assessment, useful to evaluate the areas in which focalize the attention for a micro-scale risk assessment.

The **fourth** possible future develop regard the possibility of using VISK (with meso- and micro-scale approach) to the risk assessment of other natural disaster as landslides or earthquakes.

References

- [I] Jonkman S.N., Vrijling J.K., and Vrouwenvelder A.C.W.M., *Method for the estimation of loss of life due to floods: a literature review and a proposal for a new method*. Natural Hazards, 2008. 46: p. 353-389.
- [II] FEMA, *Manual Coastal Construction*. 2000, Federal Emergency Management Agency: Washington, D.C.
- [III] De Risi R., *A probabilistic bi-scale framework for urban flood risk assessment*. Ph.D Thesis, 2013.
- [IV] De Risi R., Jalayer F., Iervolino I., Manfredi G., Carozza S., *VISK: a gis-compatible platform for micro-scale assessment of flooding risk in urban areas*. COMPDYN 2013.
- [V] Box G.E.P. and Tiao F.C., *Bayesian Inference in Statistical Analysis*, ed. W. Interscience. 1992: John Wiley & Sons, Inc.
- [VI] Benjamin J.R. and Cornell C.A., *Probability, Statistics, and Decision for Civil Engineers*. 1970: McGraw-Hill, New York.
- [VII] Shome N., *Probabilistic seismic demand analysis of nonlinear structures*. RMS Program. 1999, Stanford University.
- [VIII] Jalayer F., Elefante L., Iervolino I., and Manfredi G., *Knowledge-based performance assessment of existing RC buildings*. Journal of Earthquake Engineering, 2011. **15**(3): p. 362-389.
- [IX] Papadimitriou C., Beck J.L., and Katafygiotis L.S., *Updating robust reliability using structural test data*. Probabilistic Engineering Mechanics, 2001. **16**(2): p. 103-113.
- [X] De Risi R., Jalayer F., Iervolino I., Kyessi A., Mbuya E., Yeshitela K., and Yonas N., *Guidelines for vulnerability assessment and reinforcement measure of adobe houses*, deliverable in CLUVA project – Climate Change and Urban Vulnerability in Africa. 2012.
- [XI] Jaynes E.T., *Probability theory: The logic of science*. 2003: Cambridge University Press.

List of figures

FIGURE 2. 1: ACQUISITION OF DATA REGARDING BUILDINGS FOOTPRINT.....	24
FIGURE 2. 2: HYDROGRAPHIC BASIN MODELLING PROCEDURE.	25
FIGURE 2. 3: THE SCHEMATIC DIAGRAM OF A HYDROGRAPHIC BASIN.	25
FIGURE 2. 4: GRAPHICAL REPRESENTATION OF THE SPATIAL INTERPOLATION FOR POINT G.	27
FIGURE 2. 5: A) HAZARD CURVES; B) FLOOD HEIGHT VERSUS FLOOD VELOCITY POWER-LAW RELATION.	28
FIGURE 2. 6: A) LOGIC TREE FOR THE WATERPROOFNESS, B) LOGIC TREE FOR THE MODEL GENERATION.	31
FIGURE 2. 7: PROCEDURE USED TO VULNERABILITY ASSESSMENT.....	32
FIGURE 2. 8: A) REAL VELOCITY PROFILE; B) APPROXIMATE VELOCITY PROFILE.	34
FIGURE 2. 9: HYDROSTATIC AND HYDRODYNAMIC PRESSURE PROFILE FOR TWO DIFFERENT PAIRS OF PARAMETERS: (A) LOW FLOODING HEIGHT AND LOW VELOCITY; (B) LOW FLOODING HEIGHT AND HIGH VELOCITY.	35
FIGURE 2. 10: VARIOUS MODELS OF WALL	36
FIGURE 2. 11: ZONES OF PANEL IN WHICH IS SEARCHED THE CRITICAL SECTION.	37
FIGURE 2. 12: EVALUATION OF CRITICAL FLOODING HEIGHT IN VARIOUS SITUATIONS CORRESPONDING TO POSSIBLE MONTE CARLO EXTRACTIONS.	39
FIGURE 2. 13 - SCHEMATIC DIAGRAM OF: A) STEP FUNCTION FOR SE; B) LOGNORMAL CDF FOR SE; C) THREE- PARAMETERS CDF FOR SE; D) STEP FUNCTION FOR LS; E) LOGNORMAL CDF FOR LS; F) THREE-PARAMETERS CDF FOR LS.	41
 FIGURE 3. 1: LAYOUT OF VISK.....	48
FIGURE 3. 2 – (A): HAZARD DATA ON THE MAP VIEWED AS SURF; (B): HAZARD CURVES.....	51
FIGURE 3. 3 - DISTRIBUTION TYPES: A) NORMAL DISTRIBUTION; B) LOGNORMAL DISTRIBUTION; C) UNIFORM DISTRIBUTION.	54
FIGURE 3. 4: LOGIC TREE OF VISK GLOBAL PROCEDURE.	55
FIGURE 3. 5: VISK STRUCTURAL ANALYSIS FLOWCHART.....	58
FIGURE 3. 6: VISK FRAGILITY EVALUATION PROCEDURE.	61
FIGURE 3. 7: EXAMPLE OF VISK ROBUST FRAGILITY CURVE.	62
FIGURE 3. 8 - CUSTOM FRAGILITY CURVES: A) NORMAL CDF; B) LOGNORMAL CDF; C) NOMINAL STEP FUNCTION; D) TOTALLY CUSTOM FRAGILITY CURVE.	63
 FIGURE 4. 1: RAINFALL PROBABILITY CURVES FOR DSM CITY WITH AND WITHOUT CLIMATE CHANGE EFFECTS.....	67
FIGURE 4. 2: MIZIMBAZI CATCHMENTS.....	67
FIGURE 4. 3: HYDROGRAPHS EVALUATED FOR CATCHMENT 1	68
FIGURE 4. 4: OVERLAYING REPRESENTATIVE (MEAN AND MEAN +/- STANDARD DEVIATION) HAZARD CURVES OBTAINED BASED ON, HISTORICAL DATA (BLUE CURVES) AND CLIMATE PROJECTIONS (RED CURVES).	69
FIGURE 4. 5 – INUNDATION PROFILES FOR DIFFERENT RETURN PERIODS, BASED ON HISTORICAL DATA, IN TERMS OF H _{MAX} : A) T _R =2 YEARS, B) T _R =10 YEARS, C) T _R =30 YEARS, D) T _R =50 YEARS, E) T _R =100 YEARS, F) T _R =300 YEARS.	70

List of figures

FIGURE 4. 6 – INUNDATION PROFILES FOR DIFFERENT RETURN PERIODS, BASED ON HISTORICAL DATA, IN TERMS OF V_{MAX} : A) $T_R=2$ YEARS, B) $T_R=10$ YEARS, C) $T_R=30$ YEARS, D) $T_R=50$ YEARS, E) $T_R=100$ YEARS, F) $T_R=300$ YEARS	71
FIGURE 4. 7: PORTFOLIO OF THE BUILDINGS STUDIED IN SUNA.	72
FIGURE 4. 8: THREE ALTERNATIVE POSSIBILITIES FOR ESTIMATING THE PROBABILITY THAT THE BUILDINGS HAS A PLATFORM.....	74
FIGURE 4. 9 - ROBUST FRAGILITY CURVES AT SE LIMIT STATE: (I) 10 SIMULATIONS; (II) 50 SIMULATIONS; (III) 100 SIMULATIONS.....	77
FIGURE 4. 10 - ROBUST FRAGILITY CURVES AT CO LIMIT STATE: (I) 10 SIMULATIONS; (II) 50 SIMULATIONS; (III) 100 SIMULATIONS.....	78
FIGURE 4. 11 – OVERLAY OF THE MEDIAN FRAGILITY FOR THE THREE LIMIT STATE CONSIDERED FOR TWO TYPOLOGY OF EXTRACTION WITH 10 ANALYSIS SIMULATIONS.....	79
FIGURE 4. 12 – OVERLAY OF THE MEDIAN FRAGILITY FOR THE THREE LIMIT STATE CONSIDERED FOR TWO TYPOLOGY OF EXTRACTION WITH 50 ANALYSIS SIMULATIONS.....	80
FIGURE 4. 13 - ROBUST FRAGILITY CURVES AT CO LIMIT STATE OBTAINED BASED ON 50 SIMULATIONS: (LEFT) NORMAL CUMULATIVE DISTRIBUTION OF PROBABILITY; (RIGHT) LOGNORMAL CUMULATIVE DISTRIBUTION OF PROBABILITY.....	81
FIGURE 4. 14: OVERLAYING OF NORMAL, LOGNORMAL AND ECDF FRAGILITY CURVES.	82
FIGURE 4. 15: OVERLAYING OF ECDF AND CONFIDENCE INTERVAL.	82
FIGURE 4. 16 - FRAGILITY CURVES FOR THREE LOAD COMBINATION: (A) HINGED-FIXED SOLID WALL; (B) FIXED SOLID WALL.....	85
FIGURE 4. 17 - FRAGILITY CURVES FOR THREE LOAD COMBINATION: (A) HINGED-FIXED WALL WITH WINDOWS; (B) FIXED WALL WITH WINDOWS.	86
FIGURE 4. 18 - FRAGILITY CURVES FOR THREE LOAD COMBINATION: (A) HINGED-FIXED WALL WITH DOOR; (B) FIXED WALL WITH DOOR.	87
FIGURE 4. 19 - FRAGILITY CURVES FOR THREE LOAD COMBINATION: (A) HINGED-FIXED WALL WITH DOOR AND WINDOWS; (B) FIXED WALL WITH DOOR AND WINDOWS.	88
FIGURE 4. 20: GRAPHICAL DEFINITION OF THE RISK.	89
FIGURE 4. 21: ROBUST FRAGILITY CURVE AL LIFE SAFETY LIMIT STATE.	90
FIGURE 4. 22 - RISK MAPS IN TERMS OF PROBABILITY OF EXCEEDING THE LS LIMIT STATE: (A) IN 1 YEAR; (B) IN 2 YEARS; (C) IN 5 YEARS; (D) IN 25 YEARS.....	91

List of tables

TABLE 4. 1: GROWING FACTORS FOR THE DIFFERENT RETURN PERIODS (H: HISTORICAL, CC: CLIMATE CHANGE)...	66
TABLE 4. 2: CHARACTERISTICS OF MIZIMBAZI RIVER CATCHMENTS.	68
TABLE 4. 3: CEMENT STABILIZED BLOCKS AVAILABLE IN LITERATURE [X].....	73
TABLE 4. 4: STRUCTURAL DETAILING PARAMETERS EXPRESSED AS DISCRETE BINARY UNCERTAIN VARIABLES.....	74
TABLE 4. 5: CONTINUOUS UNCERTAIN PARAMETERS RELATED TO BUILDINGS GEOMETRY.....	75
TABLE 4. 6: CONTINUOUS UNCERTAIN PARAMETERS RELATED TO MECHANICAL PROPERTIES.	75
TABLE 4. 7: CONTINUOUS UNCERTAIN PARAMETERS RELATED TO LOADING PARAMETERS.	75
TABLE 4. 8: OTHER PARAMETERS TO ANALYSIS.	76
TABLE 4. 9: STRUCTURAL DETAILING PARAMETERS TO HAVE A WATERPROOF BUILDING MODELS.....	83
TABLE 4. 10: WALL DETAILING TO FIX "SOLID WALL" IN VISK STRUCTURAL MODEL.	84
TABLE 4. 11: WALL DETAILING TO FIX "WALL WITH DOOR" IN VISK STRUCTURAL MODEL.	84
TABLE 4. 12: WALL DETAILING TO FIX "WALL WITH WINDOWS" IN VISK STRUCTURAL MODEL.	84
TABLE 4. 13: WALL DETAILING TO FIX "WALL WITH DOOR AND WINDOWS" IN VISK STRUCTURAL MODEL.	84
TABLE 4. 14: PEOPLE AT LIFE RISK AND FINANCIAL LOSSES.	91